Das NLRP3-Inflammasom in experimenteller und humaner Temporallappenepilepsie

Inaugural-Dissertation

zur Erlangung des Doktorgrades

der Hohen Medizinischen Fakultät

der Rheinischen Friedrich-Wilhelms-Universität

Bonn

Malin Sarah Pohlentz

aus Bonn

2024

Angefertigt mit der Genehmigung

der Medizinischen Fakultät der Universität Bonn

1. Gutachter: Prof. Dr. Albert Johann Becker
2. Gutachter: Prof. Dr. Hemmen Sabir

Tag der Mündlichen Prüfung: 29.08.2024

Aus dem Institut für Neuropathologie

Direktor: Prof. Dr. med. Torsten Pietsch

Inhaltsverzeichnis

Abkürzungsverzeichnis

ANOVA	Varianzanalyse *(ANalysis Of VAriance)*
DNA	Desoxyribonukleinsäure (desoxyribonucleic acid)
RNA	Ribonukleinsäure (ribonucleic acid)
mRNA	Messenger-RNA (messenger ribonucleic acid)
TLE	Temporallappenepilepsie
SE	Status epilepticus
NLRP3	NOD-Like Receptor Protein 3
ASC	Apoptosis-Associated Speck-Like Protein
CASP1	Caspase 1
TLR4	Toll-Like-Receptor 4
HS	Hippocampus-Sklerose
LA	Läsion-assoziiert
GFAP	Glial fibrillary protein
NeuN	Neuronal nuclei
IBA1	Ionized calcium-binding adapter molecule 1
IL1B	Interleukin 1 beta
IL18	Interleukin 18
DAB	Diaminobenzidin
EEG	Elektroencephalogramm
KA	Kainat
NFκB	Nuclear Factor κB
PCR	Polymerase-Kettenreaktion (polymerase chain reaction)
RT-PCR	Realtime-PCR

1. Deutsche Zusammenfassung

1.1 Einleitung

Die häufigste Form der fokalen Epilepsie bei Erwachsenen ist die Temporallappenepilepsie (TLE) (Asadi-Pooya *et al.*, 2017). Die aktuell zur Verfügung stehenden Antiepileptika bewirken bei einem Teil der TLE-Patienten keine Anfallskontrolle (Asadi-Pooya *et al.*, 2017). Daher ist bei vielen Patienten mit arzneimittelrefraktärer TLE eine chirurgische Entfernung des epileptogenen Herdes die einzige therapeutische Möglichkeit, was bei ca. 50-60 % zu einer Anfallsfreiheit führt (Vakharia *et al.*, 2018). Die histopathologische Analyse des entnommenen Gewebes zeigt bei einem Großteil der Patienten eine sogenannte Hippocampus-Sklerose (HS) (Vakharia *et al.*, 2018), die durch reaktive Astrogliose, segmentalen neuronalen Zellverlust und Mikrogliose gekennzeichnet ist (Blümcke *et al.*, 2013; Johnson *et al.*, 2016) und einen späten Zeitpunkt im Verlauf der Erkrankung darstellt.

In TLE-Mausmodellen, in denen durch exzitotoxische Substanzen wie Pilocarpin oder Kainat (KA) ein Status epilepticus (SE) ausgelöst wird, kann das beschriebene Läsionsmuster sowie die Entwicklung chronisch rezidivierender Anfälle reproduziert werden. So bietet sich die Möglichkeit im Tierversuch den pathogenetischen Prozess, welcher zur Entwicklung chronisch wiederkehrender Anfälle führt, genauer zu untersuchen und neue therapeutische Ansätze zu entwickeln. Dieser Prozess, der sich auf molekularer, zellulärer und physiologischer Ebene vollzieht, wird als Epileptogenese bezeichnet (Becker, 2018).

Zahlreiche Studien legen eine enge Verknüpfung zwischen aseptischen Entzündungsreaktionen und der Epileptogenese nahe (Maroso *et al.*, 2010; Vezzani and Rüegg, 2011). In Tierversuchen konnte durch die Blockade von proinflammatorischen Signalmolekülen ein positiver Einfluss auf den Krankheitsverlauf erzielt werden (Maroso *et al.*, 2011; Meng *et al.*, 2014; Vezzani and Viviani, 2015; Wu *et al.*, 2020). In diesem Zusammenhang spielt unter anderem der NOD-like receptor protein 3 (NLRP3) - Signalweg (siehe Abb. 1A, Pohlentz et al., 2022) eine große Rolle. Hierbei bewirkt die Aktivierung des Toll-like-Rezeptors 4 (TLR4) über eine Translokation von Nuclear Factor

κB (NFκB) die Transkription von Pro-Interleukin-1-beta (Pro-Il1b) und Nlrp3 (Bauernfeind *et al.*, 2009). Ein weiterer intrazellulärer Trigger (z.B. Akkumulation reaktiver Sauerstoffmoleküle oder ein Abfall der Kaliumkonzentration) induziert dann die Bildung und Aktivierung des NLRP3-Inflammasoms (Schroder and Tschopp, 2010), das aus NLRP3, dem Apoptose-assoziierten Speck-like-Protein (ASC) und Pro-Caspase-1 besteht. Das aktivierte Inflammasom wiederum spaltet und aktiviert Pro-Caspase-1. Caspase-1 bewirkt daraufhin die Spaltung von Pro-IL1B und damit die Aktivierung und Freisetzung von Interleukin 1 beta (IL1B) (Bergsbaken *et al.*, 2011).

Moleküle des NLRP3-Siganlwegs zeigten sich in reseziertem hippocampalem Gewebe von TLE-Patienten erhöht exprimiert (Crespel *et al.*, 2002; Leal *et al.*, 2017; Wu *et al.*, 2020; Cristina de Brito Toscano *et al.*, 2021). In experimenteller TLE konnte die Hemmung einzelner Bestandteile der NLRP3-Kaskade die Anfallshäufigkeit und Anfallsschwere verringern und die Neuroinflammation reduzieren (Vezzani *et al.*, 2000; Vezzani, Balosso and Ravizza, 2008; Bauernfeind *et al.*, 2009; Iori *et al.*, 2017; Wu *et al.*, 2020). So wurde unter anderem durch kleine interferierende RNA-Moleküle (Small Interfering Ribonucleic Acids, siRNAs) vermittelte Ausschaltung von *Nlrp3* ein neuroprotektiver Effekt erzielt und das Einsetzen der chronisch rezidivierenden Anfälle verzögert sowie die Anfallsdauer und -häufigkeit vermindert (Meng *et al.*, 2014). In NLRP3-Knockout Mäusen zeigte sich eine Reduktion des IL1B-Spiegels im peripheren Blut sowie eine verminderte neuronale Nekrose und Apoptose eine Woche nach Pilocarpin-induziertem SE (Wu *et al.*, 2020).

1.1.1 Fragestellung

In dieser Arbeit untersuchen wir die Aktivierung des NLRP3-Signalwegs und die IL1B-Expression in zwei Mausmodellen für pharmakoresistente TLE, um den Zusammenhang zwischen diesen Prozessen und der Neuroinflammation während der Epileptogenese und in chronischer Epilespie näher aufzuschlüsseln.

1.2 Material und Methoden

Tiere

Alle Tierversuche wurden gemäß den Richtlinien des Universitätsklinikums Bonn, der Tierschutzkommission und der Europäischen Richtlinie 2010/63/EU sowie den ARRIVE-Richtlinien durchgeführt, um Schmerzen und Leiden der Tiere sowie die Anzahl der verwendeten Tiere zu minimieren. Die Mäuse wurden in einer Umgebung mit kontrollierter Feuchtigkeit (55 ± 10 %) und Temperatur (22 ± 2 °C) unter einem 12-Stunden-Licht-Dunkel-Zyklus (Lichtzyklus 7 bis 19 Uhr) gehalten, mit Wasser und Futter ad libitum sowie Nistmaterial (Nestlets, Ancare, USA). Vor jeder Behandlung hatten die Mäuse mindestens sieben Tage Zeit zur Akklimatisierung.

Auslösung von chronischer Epilepsie durch suprahippocampale Kainsäure-Injektion

Wie zuvor beschrieben, wurden männliche C57Bl6/N-Mäuse (Charles River; ~60 Tage alt, Gewicht ≥ 20 g) zur Induktion der chronischen Epilepsie verwendet. Dazu wurden nach Betäubung mit 16 mg/kg Xylazin (Ceva Tiergesundheit, Deutschland) und 100 mg/kg Ketamin (i.p., Ketamin 10%, WDT, Deutschland) 70 nl Kainsäure (20 mM in 0,9% NaCl, Tocris) über 2 Minuten unilateral in die CA1-Region des linken dorsalen Hippocampus (stereotaktische Koordinaten relativ zu Bregma: -2 anterioposterior, -1,5 mediolateral, -1,4 dorsoventral) mit einer Nanofil-Spritze (WPI) und Mikropumpe (WPI) appliziert (Pitsch et al., 2019). Kontrollmäusen (Nicht-SE) wurde auf die gleiche Weise 70 nl 0,9% NaCl injiziert. Alle operierten Mäuse erhielten vor und einmal täglich für drei Tage nach der Operation ein Analgetikum (5 mg/kg Ketoprofen, s.c.; Gabrilen, Trommsdorff GmbH & Co. KG). Diese Methode induziert in 100% der Fälle einen SE ohne Todesfälle (Pitsch et al., 2019). Alle Tiere entwickelten chronische fokale bis bilaterale tonisch-klonische Anfälle (10d, 28d nach SE).

Induktion von chronischer Epilepsie durch systemische Pilocarpin-Injektion

Zur SE-Induktion wurden männliche C57Bl6/N-Mäuse (Charles River; ~60 Tage alt, Gewicht ≥ 20 g) gemäß früheren Veröffentlichungen (Pitsch et al., 2012a, 2017) 20 Minuten nach einer Vorbehandlung mit 1 mg/kg Scopolaminmethylnitrat (Sigma) subkutan mit 335 mg/kg Pilocarpinhydrochlorid (Sigma) injiziert. Vierzig Minuten nach

Beginn des SE erhielten die Tiere Diazepam (4 mg/kg, s.c.; Ratiopharm). Kontrolltiere (ohne SE) erhielten Kochsalzlösung anstelle von Pilocarpin. Der SE wurde anhand eines modifizierten Anfallsschemas eindeutig identifiziert und als anhaltende, kontinuierliche Konvulsionen mit Haltungsverlust definiert (Pitsch et al., 2012b, 2017). Nur die Tiere, die SE entwickelten, wurden für die weitere Analyse verwendet. Alle SE-erfahrenen Tiere zeigten in späteren Modellstadien (5d-, 10d-, 28d-Gruppe) fokale bis bilaterale tonisch-klonische Krampfanfälle.

Telemetrische Video-/EEG-Überwachung

Nach KA- oder Pilocarpin-induziertem SE wurden kontinuierlich semiologische Merkmale mittels telemetrischem EEG und Videoüberwachung untersucht. Die Verfahren zur EEG-Implantation, postoperativen Pflege, Überwachung und Anfallsklassifizierung sind in Pitsch et al. (2017, 2019) detailliert beschrieben. Zwei Wochen vor der Pilocarpin-Injektion oder unmittelbar nach der KA-Injektion wurde eine EEG-Elektrode (Bregma: -2 AP, -1,5 ML) implantiert, verbunden mit subkutanen Sendern (ETA-F20, DSI). Eine Edelstahlschraube an der Kleinhirnrinde (Bregma: -6 AP) diente als Referenzelektrode. Die korrekte Elektrodenplatzierung wurde histologisch überprüft. EEG-Daten wurden ab der Implantation kontinuierlich mit 1 kHz aufgezeichnet und mittels NeuroScore v3.2 (DSI) analysiert. Anfälle wurden anhand gleichzeitiger Videoaufzeichnungen klassifiziert (Pitsch et al., 2017, 2019).

mRNA-Isolierung bei Mäusen, RT-PCR-Quantifizierung in Echtzeit, histopathologische Analyse, Zellquantifizierung

mRNA wurde aus der lysierten CA1-Region des Hippocampus mittels magnetischer Beads (mRNA Direct™ Micro Kit, Invitrogen) isoliert und in cDNA umgewandelt (RevertAid H Minus First Strand cDNA Synthesis Kit, Thermo Scientific; Pitsch et al., 2019). Die Transkripte der Gene wurden durch RT-PCR mit dem CFX384 Touch Real-Time PCR Detection System (Biorad) und der ΔΔCt-Methode quantifiziert (RT-PCR-Zyklen: 2 min bei 50 °C, 10 min bei 95 °C, 40 Zyklen von 15 s bei 95 °C, 30 s bei 60 °C und 30 s bei 72 °C.). PCR-Proben für ASC und NFκB2 enthielten 3 µl Maxima Probe/ROX qPCR Master Mix (Thermo Scientific), 0,3 µl TaqMan™ Gene Expression Assay (Thermo Scientific), 1,7 µl RNase-freies Wasser und 2 µl cDNA. Andere PCR-

Proben enthielten 3,125 µl Maxima SYBR Green/ROX qPCR Master Mix (Thermo Scientific), 0,3 µM Primer (Tab. 1), 1,5 µl cDNA und 1,5 µl Wasser. Daten der linken und rechten CA1-Region wurden gepoolt, da zwischen den Hemisphären keine signifikanten Unterschiede festgestellt wurden (siehe Abb. 1A).

Tab. 1: Oligonukleotid-Primer für RT-PCR

Gen	FW-Primer	RV-Primer
Nlrp3	AATGCCCTTGGAGACACAGG	ATTCCAGCAGCTGTGTGAGG
Casp1	GGACCCTCAAGTTTTGCCGCT	ATGAGGGCAAGACGTGTACG
Iba1	TCAGAATGATGCTGGGCAAG	GACCAGTTGGCCTCTTGTGT
Gfap	AGAAAACCGCATCACCATTC	TCTTGAGGTGGCCTTCTGAC
Il1b	CACTACAGGCTCCGAGATGA	TTTGTCGTTGCTTGGTTCTC
Tlr4	CCAATTTTTCAGAACTTCAGTGG	AGAGGTGGTGTAAGCCATGC
β-Actin	ACCGTGTGAAAAGATGACCCAGA	ATGGGCACAGTGTGTGGGTGA

Für Immunhistochemie wurden die Mäuse unter Isofluran-Narkose enthauptet, die Gehirne über Nacht in 4 % PFA fixiert und in Paraffin eingebettet. Koronarschnitte (4 µm) wurden für GFAP (NeuroMab, 1:250), NeuN (Millipore, 1:500), IBA1 (Wako, 1:1000) und IL1B (abcam, 1:100) verwendet (Pitsch et al., 2019). Paraffinschnitte wurden entparaffiniert, gewaschen, Antigene in Zitronensäure (10 mM, pH 6,0) bei 90 °C für 8 Minuten demaskiert, und bei 37 °C in PBS-Puffer mit 10 % Ziegenserum und 1 % fetalem Kälberserum blockiert. Nach der Inkubation mit primären Antikörpern über Nacht bei 4 °C wurden die Schnitte mit sekundären Antikörpern (Life technologies, 1:100) und DAPI (Sigma, 1:100.000) in Blocking-Puffer inkubiert, gewaschen und mit Mowiol 4-88 (Roth) montiert. Für die halbquantitative Analyse von Mikroglia und Astrozyten wurde eine DAB-Färbung (3,3′-Diamino-Benzidin) verwendet. Nach Blockierung mit 5 % Ziegenserum in PBS bei 37 °C wurden die Schnitte mit GFAP (Sigma, 1:500) und IBA1 (Wako, 1:1000) über Nacht bei 4 °C inkubiert. Nach Waschen und Inkubation mit

biotinylierten sekundären Antikörpern (Vector Laboratories, 1:200) bei 37 °C, wurden die Objektträger gemäß dem Herstellerprotokoll (Sigmafast, Merck) verarbeitet und mit Mowiol 4-88 (Roth) eingeschlossen. Nicht fluoreszierende Bilder wurden mit einem Mikroskop (BZ-X, Keyence) und fluoreszierende Bilder mit einem konfokalen Mikroskop (Nikon, Eclipse Ti) aufgenommen. Zellquantifizierung erfolgte mit Fiji (ImageJ) durch Farbdekonvolution und Anwendung eines globalen Schwellenwerts auf den DAB-Kanal zur Erstellung binärer Bilder. Daten wurden als Flächenanteil (0-100) extrahiert. Pro Maus wurden drei Abschnitte (zwischen -1,6 mm und -2,1 mm anterio-posterior relativ zum Bregma) und innerhalb jedes Abschnitts drei benachbarte Felder von CA1 quantifiziert.

TLE-Patienten, mRNA-Sequenzierung und histopathologische Analyse

Genexpressionsanalysen wurden an hippocampalem Biopsiegewebe von Patienten mit Hippocampus-Sklerose (HS, n=78) und läsionsassoziierter chronischer TLE (n=34) durchgeführt, die sich aufgrund von Pharmakoresistenz einer Operation am Universitätsklinikum Bonn unterzogen (Van Loo et al., 2015). Alle Patienten hatten Anfälle aus dem mesialen Temporallappen (Kral et al., 2002). HS war durch segmentalen neuronalen Zellverlust, Astrogliose und Mikrogliaaktivierung gekennzeichnet. Kontroll-Hippocampi zeigten keine segmentalen neuronalen Zellverluste, jedoch Astrogliose und Mikrogliaaktivierung, passend zu Läsionen wie kortikaler Dysplasie oder Epilepsie-assoziierten Tumoren. Diagnosen wurden nach internationalen Kriterien gestellt (Becker et al., 2003; Blümcke et al., 2007). Alle Verfahren erfolgten gemäß der Deklaration von Helsinki und wurden von der Ethikkommission des Universitätsklinikums Bonn genehmigt (222/16). Alle Patienten gaben schriftliches Einverständnis. mRNA-Analysen für Nlrp3, Casp1, Tlr4, NfkB2, Il1b, Il18, Gfap und Iba1 folgten einem bereits beschriebenen Verfahren (Pernhorst et al., 2013). 750 ng cRNA wurden aus Hippocampus-RNA hergestellt und auf Human HT-12 v3 Expression BeadChips (Illumina) hybridisiert. Datenanalyse erfolgte mit GenomeStudio und Illumina BeadStudio Software Suite, normalisiert durch Quantilnormalisierung und Hintergrundsubtraktion.

Tab. 2: Allgemeine klinische Daten (modifiziert nach: S1 Table, Pohlentz et al., 2022), Engel IA = vollständig anfallsfrei, Engel IVB = keine Anfallsfreiheit

	läsionsassoziiert	(n)	HS	(n)
Anzahl der Patienten	34		78	
Geschlecht (w/m)	64.7% vs. 35.3%	34	47.4 % vs. 52.6 %	78
Alter bei Anfallsbeginn	10.7 ± 1.5	34	11.5 ± 1.5	78
Anfallsfrequenz / Monat	16.5 ± 6.0	34	13.9 ± 2.9	78
Medikamentöse Therapie*	17.6 % vs. 35.3 % vs. 47.1 %	34	20.5 % vs. 37.2 % vs 42.3 %	78
Alter bei Operation	23.0 ± 2.8	34	35 ± 1.7	78
Postoperatives Outcome (Engel IA vs. Engel IVB)	45.5 % vs. 54.5 %	33	61.3 % vs 38.7 %	75

*Natriumkanal-Blocker Monotherapie vs. Levetiracetam Kombination vs. Kombination ohne Levetiracetam

Humanes Hirngewebe wurde über Nacht in Formaldehyd fixiert und in Paraffin eingebettet. 4 µm-Schnitte wurden für Hämatoxylin-Eosin-Färbung (H&E) und Immunhistochemie verwendet (Pitsch et al., 2007). Paraffinschnitte wurden in Xylol entparaffiniert, in absteigenden Alkoholreihen gewaschen und einem Antigen-Renaturierungs-Verfahren unterzogen. Hirnschnitte wurden in PBS-Blocking-Puffer (10 % Ziegenserum) gespült und über Nacht bei RT mit Antikörpern gegen GFAP (Dako, 1:100), NeuN (Milipore, 1:1000), IBA1 (Wako, 1:1000) oder NLRP3 (abcam, 1:100) inkubiert. DAB-Färbung erfolgte wie bei Mäuseschnitten (s.o.). Für Fluoreszenz-Immunhistochemie wurden Objektträger nach Waschen mit sekundären Antikörpern (Alexa Fluor®568, Life technologies, 1:200) und DAPI (Sigma, 1:100.000) inkubiert und mit Mowiol 4-88 (Roth) fixiert. NLRP-Expressionsmuster wurden morphologisch analysiert.

Statistische Auswertung

Die Experimente wurden randomisiert und verblindet durchgeführt. Die statistische Analyse erfolgte mit Prism 9 (GraphPad Software). Die Stichprobengröße (n) wurde durch Power-Analyse bestimmt. Zur Untersuchung der SE-Auswirkungen auf NLRP-Gene wurde ein Two-Way-ANOVA verwendet, wobei SE und Zeit nach SE die unabhängigen Variablen waren. Der Sidak-Mehrfachvergleichstest identifizierte signifikante Unterschiede zwischen Kontroll- und SE-Gruppen zu bestimmten Zeitpunkten. Der Mann-Whitney-U-Test analysierte NLRP-Genexpressionunterschiede zwischen Läsions- und Hippocampus-Sklerosestellen in menschlichen Proben.

Zur Korrelationsanalyse nutzten wir den Median der Anfallsfrequenz von drei aufeinanderfolgenden Tagen vor der mRNA-Analyse (Tag 3: Anfälle von Tag 1-3; Tag 5: Anfälle von Tag 3-5; Tag 10: Anfälle von Tag 8-10; Tag 28: Anfälle von Tag 26-28) bei KA (n=21) und Pilocarpin-induziertem SE (n=11). Die mediane Anfallshäufigkeit wurde durch lineare Regression mit der durchschnittlichen Genexpression korreliert. Statistische Ausreißer wurden durch den Grubb-Test (GraphPad) identifiziert und ausgeschlossen. Unterschiede zwischen den Mittelwerten galten bei $p<0,05$ als signifikant. Alle Ergebnisse sind als Mittelwert ± Standardabweichung angegeben. Negative Fehlerbalken, die die x-Achse überschreiten, wurden abgeschnitten.

1.3 Ergebnisse

1.3.1. Nach Status epilepticus zeigt sich eine signifikante, zeit- und modellabhängige Aktivierung von Inflammasom-assoziierten Molekülen.

Zunächst untersuchten wir die Inflammasom-bezogenen molekularen Dynamiken im Hippocampus über einen Zeitraum von vier Wochen nach systemischer Pilocarpin- und einseitiger suprahippocampaler KA-Injektion. Im Pilocarpin-Modell zeigte sich in der frühen Phase eine erhöhte Expression von *Nlrp3*, weiterer Inflammasom-Bestandteilen und der beteiligten Signalmoleküle. Die Expressionssteigerung erreichte 10 Tage nach SE ihren Höhepunkt (siehe Abb. 1B, Pohlentz et al., 2022). Während der chronisch epileptischen Phase waren die mRNA-Level aller untersuchten NLRP3-Kaskadenkomponenten nicht mehr erhöht. Auch im KA-Modell wurde eine erhöhte Expression der NLRP3-assoziierten Moleküle in der frühen Phase beobachtet (72 h und

5 d nach SE, siehe Abb. 1C, Pohlentz et al., 2022). Diese war jedoch am 10. Tag nach SE rückläufig und ohne signifikanten Unterschied zu den Kontroll-Tieren. Erst in der chronischen epileptischen Phase stieg die mRNA-Expression erneut an, ohne dass Unterschiede zwischen dem KA-injizierten und dem kontralateralen Hippocampus festzustellen waren (Abb. 1A).

In Bezug auf die nachgeschalteten Effekte des Inflammasoms untersuchten wir den zeitlichen Verlauf der Interleukin 1 beta (IL1B) Expression auf transkriptioneller und translationaler Ebene in beiden Tiermodellen. Im Pilocarpin-Modell zeigte sich eine gesteigerte Il1b-Transkription ausschließlich 10 Tage nach SE-Induktion, während die Interleukin 18 (Il18) Genexpression 72 Stunden nach SE-Induktion signifikant vermindert war (siehe Abb. 2A, Pohlentz et al., 2022). In gruppierten Neuronen wurde bereits 72 Stunden nach SE eine erhöhte Protein-Expression von IL1B nachgewiesen (siehe Abb. 2C, Pohlentz et al., 2022), die sich jedoch nach 10 Tagen auf ein geringeres Niveau reduzierte. In der chronischen Phase wurde eine Ansammlung von nicht-neuronalen Zellen mit starker IL1B-Immunoreaktivität (u.a. Astrozyten) in den Bereichen mit ausgeprägter Neurodegeneration beobachtet. Im KA-Modell hingegen wurde eine Steigerung der Il1b mRNA-Spiegel zu allen untersuchten Zeitpunkten festgestellt, während die Il18 Expression nicht signifikant verändert war (siehe Abb. 3A und 3B, Pohlentz et al., 2022). Immunhistochemische Untersuchungen zeigten in den neuronalen Zellkörpern eine granuläre IL1B-Expression während des gesamten Untersuchungszeitraums. Zusätzlich wurde eine zunehmende Expression von IL1B in nicht-neuronalen Zellen, insbesondere Astrozyten, in der dorsalen CA1-Region beobachtet, die in der chronischen Phase ihren Höhepunkt erreichte (siehe Abb. 3C und 3D, Pohlentz et al., 2022).

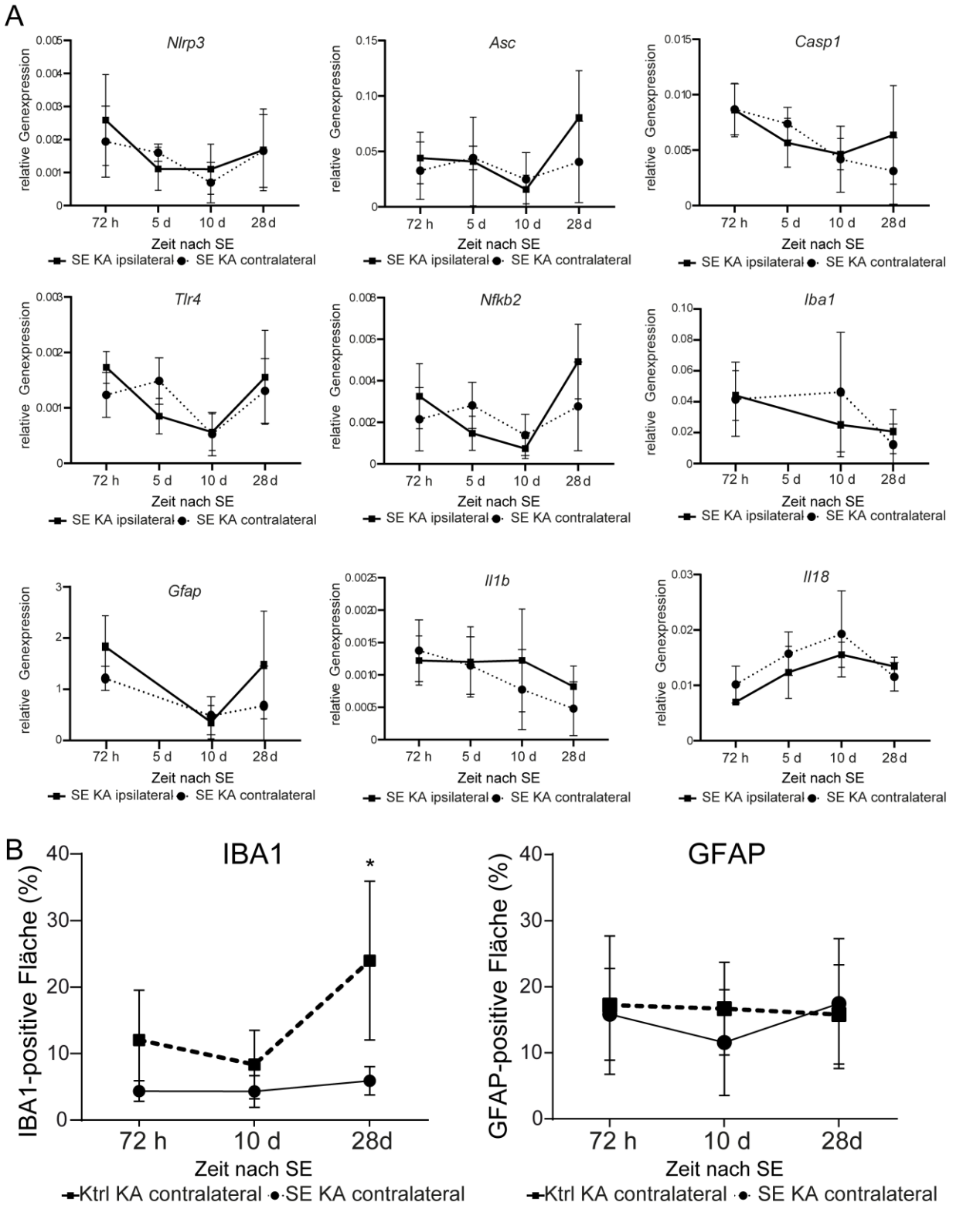

Abb. 1: Zwischen der ipsi- und kontralateralen CA1-Region nach KA-induziertem SE wurde kein Unterschied in der mRNA-Expression inflammasomaler Gene beobachtet (modifiziert nach Suppl. Fig. 1, Pohlentz et al., 2022)

(A) Relative mRNA-Spiegel (ΔΔCt-Methode) in ipsi- und kontralateralem CA1 werden 72 Stunden (n ≥ 4), 5 Tage (n ≥ 5), 10 Tage (n ≥ 4) und 28 Tage (n ≥ 6) nach Kainsäure-induziertem SE mittels Zwei-Wege-ANOVA und Sidak-Post-Hoc-Test analysiert. β-Actin dient als Housekeeping-Gen. (B) Die semiquantitative Analyse der IBA1- und GFAP-positiven Flächen zeigt im kontralateralen CA1 nahezu keine signifikanten Veränderungen (alle Gruppen n = 3), analysiert mit Zwei-Wege-ANOVA und Sidak-Post-Hoc-Test. Ein signifikanter Anstieg der Mikroglia (IBA1) wurde nur in der späten Modellphase (28 Tage) in der kontralateralen CA1-Region beobachtet. Signifikante Unterschiede zwischen den Gruppen sind mit Sternchen markiert: *p < 0.05.

1.3.2 Die entzündliche Aktivierung auf zellulärem Level folgt einem ähnlichen zeit- und modellabhängigem Muster.

Die Beteiligung von Astrozyten und Mikroglia an der Neuroinflammation wurde bereits in vielen Erkrankungen des zentralen Nervensystems inklusive der TLE nachgewiesen (Rizzi et al., 2003; Bauer et al., 2017; Leal et al., 2017). Daher untersuchten wir im Folgenden in beiden TLE-Modellen die zeitabhängige Aktivierung von Astrozyten und Mikroglia anhand der Markerproteine GFAP und IBA1 (Synonym: AIF1). Unsere Untersuchungen zeigten im Pilocarpin-Modell eine signifikante Zunahme der mRNA-Spiegel von *Gfap* und *Iba1* nach 72 Stunden, 10 Tagen und 28 Tagen nach SE (siehe Abb. 4A, Pohlentz et al., 2022). Die Fläche der IBA1- und GFAP-positiven Zellen nahm ebenfalls zu (siehe Abb. 4B, Pohlentz et al., 2022). Schon nach 72 Stunden zeigten sich einzelne aktivierte Mikroglia (siehe Abb. 4C Pohlentz et al., 2022). Im weiteren Verlauf wurde hypertrophe Mikroglia mit vielen Fortsätzen (d.h. in einem höheren Aktivierungszustand (Wyatt-Johnson et al., 2017)) beobachtet. Nach 72 Stunden zeigte sich eine milde bis moderate Astrogliose, später nahm die Anzahl der Astrozyten zu, welche jedoch schlankere Zellkörper und Zellfortsätzen und demnach einen weniger reaktiven Zustand aufwiesen.

Im KA-induzierten SE Mausmodell zeigte sich eine Zunahme der Genexpression auf mRNA-Ebene vorrangig in den frühen Zeitpunkten nach SE (*Iba1*: 72 h und 10 d, *Gfap*: 72 h, vergleiche Abb. 5A, Pohlentz et al., 2022). *Gfap* wies ein zweites Expressionsmaximum 28 Tage nach SE auf, ähnlich dem Zeitverlauf der *Nlrp3*-Expression. Die Fläche der IBA1 und GFAP-positiven Zellen in der ipsilateralen CA1-Region nahm über den Untersuchungszeitraum zu (siehe Abb. 5B, Pohlentz et al., 2022). Kontralateral hingegen war diesbezüglich kein wesentlicher Unterschied

gegenüber den Kontrollen festzustellen (Abb. 1B). Lediglich im späten Stadium (28 d post SE) nahm die Fläche der IBA1-positiven Zellen auch kontralateral zu. Immunhistochemische Färbungen zeigten ipsilateral zunehmend aktivierte Mikroglia im Verlauf des untersuchten Zeitraumes (siehe Abb. 5C, Pohlentz et al., 2022). Kontralateral nahm der Aktivierungsgrad der Mikroglia 10 Tage nach SE ab, um dann im chronischen Stadium wieder zuzunehmen (siehe Abb. 5D, Pohlentz et al., 2022). Eine milde bis moderate Astrogliose zeigte sich bereits 72 Stunden nach KA-vermittelter SE-Induktion im gesamten Hippocampus. Im weiteren Zeitverlauf war eine Zunahme der Astrogliose vor allem ipsilateral zu beobachten. Im chronischen Stadium (28 d post SE) zeigte sich eine starke Astrogliose mit kompakter Narbenbildung in der ipsilateralen CA1-Region bei moderater Astrogliose und Destruktion der gesamten Hippocampus-Formation. Kontralateral wurde eine starke Astrogliose vornehmlich in der CA1-Region bei weitestgehend erhaltenen strukturellen Verhältnissen des restlichen Hippocampus beobachtet.

1.3.3 In humanen Hippocampus-Biospieproben von Patienten mit therapierefraktärer TLE zeigt sich die Aktivierung der NLRP3-Kaskade unabhängig von der zugrundeliegenden Pathologie und dem Ausmaß der neuronalen Schädigung

In einem translationalen Versuch prüften wir, ob typische inflammasombezogene Signaturen in chronischen TLE-Hippocampi mit ausgedehnter neuronaler Schädigung auftreten. Als Vergleich zogen wir Hippocampi von läsionsassoziierter TLE (LA-TLE) heran, die chronisch epileptisch sind, jedoch keiner Epileptogenese unterlaufen sind oder HS aufweisen. Patientenproben mit therapierefraktärer TLE zeigen spezifische neuropathologische Merkmale (siehe Abb. 6A, H. & E., Pohlentz et al., 2022), mit deutlichen strukturellen Veränderungen im Vergleich zu läsionsassoziierter TLE. So weist HS-TLE einen erhöhten neuronalen Zellverlust und starke Astrogliose auf (siehe Abb. 6A und 6B, NeuN und GFAP, Pohlentz et al., 2022). Mikroglia-Infiltration wurde in beiden Gruppen beobachtet (siehe Abb 6B, IBA1, Pohlentz et al., 2022) und auch die NLRP3-Proteinexpression zeigte keine Unterschiede (siehe Abb. 6C, Pohlentz et al., 2022).

In einer weiteren Analyse verglichen wir die transkriptionelle Aktivierung zwischen HS-TLE und LA-TLE mittels mRNA-Sequenzierungen (siehe Abb. 6D, Pohlentz et al., 2022).

HS-TLE wies eine erhöhte *Gfap*-Expression auf, was reaktive Astrozyten anzeigt. *Iba1*-Expression für Mikroglia unterschied sich nicht signifikant. Die meisten NLRP3-Signalwegkomponenten zeigten ebenfalls keine Unterschiede, eine Ausnahme bildete *Tlr4*-mRNA, die in HS-TLE stärker exprimiert war.

1.4 Diskussion

In dieser Studie analysierten wir in zwei verschiedenen SE-induzierten TLE Mausmodellen die zeitliche Dynamik proinflammatorischer Prozesse anhand des NLRP3-Signalweges sowie auf zellulärer Ebene. Im Gegensatz zu vorherigen Studien, die in Tierversuchen eine Aktivierung des NLRP3-Signalwegs als eine akute proinflammatorische Antwort auf einen chemokonvulsiv oder elektrisch getriggerten SE untersuchten (Meng *et al.*, 2014; Jiang *et al.*, 2015; Wu *et al.*, 2020; Yue *et al.*, 2020), beobachteten wir die Genexpression und zelluläre Aktivierung über einen Zeitraum von vier Wochen nach SE-Induktion. Die verwendeten Mausmodelle (systemisches Pilocarpin- und suprahippocampales KA-Modell) replizieren die neuropathologischen Aspekte, die für die häufigste Form der TLE charakteristisch sind: HS, neuronaler Zelltod sowie einen strukturellen Umbau (Becker, 2018). Unsere Ergebnisse deuten auf eine zeitabhängige Aktivierung des NLRP3-Signalweges hin, die spezifisch für den jeweiligen Stimulus sind. Nach systemischer Gabe von Pilocarpin zeigte sich eine anhaltendende Entzündungsreaktion. Hier war eine signifikant erhöhte Expression Inflammasom-spezifischer Moleküle 72 Stunden und 10 Tage nach SE-Induktion nachweisbar, welche in der chronischen Phase (28 d post SE) jedoch nicht mehr zu detektieren war. Im Gegensatz dazu zeigte sich nach KA-induziertem SE ein biphasischer Verlauf der Entzündungsreaktion, mit einer Expressionssteigerung in der frühen Phase nach SE-Induktion (72 h) sowie in der chronischen Phase (28 d post SE). Es ist nicht davon auszugehen, dass der zweite Anstieg der proinflammatorischen mRNA-Level mit einer erhöhten Anfallsfrequenz assoziiert ist, da vorherige Studien zeigten, dass in diesem Modell die Anfallsfrequenz bis sechs Wochen nach SE-Induktion stabil bleibt (Pitsch, et al., 2019).

In Übereinstimmung mit früheren Studien zu Pilocarpin-induziertem SE bei Ratten (Ravizza *et al.*, 2008) wiesen wir eine IL1B-Immunoreaktivität im gesamten

Untersuchungszeitraum nach (72 h – 28 d post SE). Interessanterweise beobachteten wir in beiden Modellen eine zeitabhängige Änderung der zellulären Expression. Während in der frühen Phase nach SE-Induktion (72 h post SE) IL1B hauptsächlich in Neuronen lokalisiert war, wurde zu späteren Zeitpunkten (10 d und 28 d post SE) eine Expression vornehmlich in Glia-Zellen beobachtet. Die frühe neuronale Expression werten wir am ehesten als Effekt exzitotoxischer Wirkung. Im KA-Modell zeigte sich eine diffuse Verteilung der neuronalen IL1B-Expression über die gesamte CA1-Region. Wir vermuten, dass eine KA-Applikation über dem Hippocampus einen direkten (exzito-) toxischen Effekt auf eine große Anzahl Neurone in einem breiten Areal der CA1-Region hat. Dies wiederrum bewirkt eine diffuse neuronale IL1B-Expression, die in Summe stark genug ist, um auch über mRNA-Quantifizierung erfasst zu werden. Nach systemischer Pilocarpin-Injektion hingegen ist von einem indirekten toxischen Effekt über Hyperexzitation auszugehen, der zu einem gruppierten Schädigungsmuster führt. In vorherigen Studien wurde segmentaler neuronaler Zellverlust im Pilocarpin-Modell bereits zwei Tage nach SE-Induktion beobachtet (Mello *et al.*, 1993; Covolan and Mello, 2000; Becker *et al.*, 2008) Wir zeigten eine lokalisierte Expression von IL1B geclustert in einer kleinen Anzahl Neurone in der CA1 Region. Diese gruppierte Expression wurde bereits in früheren Studien nach elektrisch-induziertem SE in Ratten beobachtet (De Simoni et al., 2000). Da die IL1B-Expression im Pilocarpin-Modell auf einzelne Neurone beschränkt ist, kann die Überexpression auf mRNA-Level am ehesten aus technischen Gründen (bei Verdünnungseffekten) nicht nachgewiesen werden.

In einem translationalen Versuch analysierten wir die Expression von inflammasom-assoziierten Molekülen in Gewebeproben von Patienten mit pharmakoresistenter TLE und verglichen sie mit Patienten, die läsionsassoziierter TLE ohne segmentale Neurodegeneration aufwiesen. Frühere Studien wiesen auf eine erhöhte Expression von NLRP3 und verwandten Molekülen im Hippocampus von HS-TLE-Patienten hin (Wu *et al.*, 2020; Yue *et al.*, 2020; Cristina de Brito Toscano *et al.*, 2021). In unserer aktuellen Studie stellten wir fest, dass die Expression von Tlr4 in HS-Hippocampi im Vergleich zu Hippocampi mit Läsionen signifikant erhöht war, was auf die Bedeutung der HMGB1-TLR4-Achse für diese spezielle TLE-Form hinweist. Die restlichen inflammasomalen Signalmoleküle zeigten keine signifikanten Unterschiede. Unsere Ergebnisse deuten darauf hin, dass in chronischen TLE-Hippocampi, die einer Epileptogenese unterlaufen

sind, eine weitgehend einheitliche Expression der Schlüsselkomponenten des Inflammasoms vorliegt, die unabhängig von neurodegenerativen Veränderungen und dem Grad der Astrogliose ist. Dies deckt sich mit unseren Befunden im KA-Mausmodell, in denen keine Expressionsunterschiede der NLRP3-assoziierten Moleküle zwischen der ipsilateralen CA1-Region (starke Astrogliose mit kompakter Narbenbildung) und kontralateralen CA1-Region (moderate Astrogliose) nachgewiesen wurden. Darüber hinaus legen unsere Daten nahe, dass im chronischen Stadium der Krankheit die Anfallsaktivität möglicherweise die wichtigste Triebkraft für die proinflammatorische Inflammasom-Signalgebung darstellt, während der Untergang von Neuronen und die damit verbundene Freisetzung von Signalstoffen weniger entscheidend zu sein scheint. Diese neuen Erkenntnisse tragen zum Verständnis der molekularen Mechanismen bei, die der Pathologie der TLE zugrunde liegen.

Die wichtigsten zellulären Komponenten für die Initiierung und Aufrechterhaltung der sterilen Neuroinflammation sind Mikroglia und Astrozyten. Im aktivierten Zustand werden sie mit der Freisetzung von proinflammatorischen Zytokinen bei menschlicher und experimenteller TLE in Verbindung gebracht (Vezzani *et al.*, 2002; Rizzi *et al.*, 2003; Bauer *et al.*, 2017; Leal *et al.*, 2017). Bedner et al. 2015 und Zhao et al. 2018 demonstrierten, dass diese Zelltypen in experimentellen Modellen zur Epileptogenese beitragen. Wir analysierten die Expression der Markerproteine IBA1 und GFAP sowohl bei chronischer humaner TLE als auch im Zeitverlauf in unseren Tiermodellen. Im Vergleich zwischen humaner HS- und läsionsassoziierter TLE zeigten Patienten mit HS eine stärkere strukturelle Reorganisation, Neurodegeneration und Astrogliose. Die Mikroglia-Infiltration unterschied sich jedoch nicht zwischen den beiden Gruppen. In den Tiermodellen zeigten sich die höchsten mRNA-Spiegel und die aktivierteste Zellmorphologie 10 Tage nach Pilocarpin-induziertem SE. Im KA-Modell wurden im chronischen Stadium dicht gepackte und stark aktivierte Mikroglia und Astrozyten sowie die höchsten mRNA-Level beobachtet. Diese Ergebnisse stehen bezüglich des zeitlichen Verlaufes im Einklang mit den zuvor von uns erhobenen Daten zu den NLRP3-spezifischen molekularen Veränderung. In einer Studie, welche sich auf noch spätere Zeitpunkte im suprahippocampalen KA-Modell konzentrierte, konnte gezeigt werden, dass astrozytenbezogene pathogene Veränderungen bis zu neun Monate nach SE-Induktion fortschreiten (Bedner *et al.*, 2015). Im KA-Modell beobachteten wir an Tag

10 eine zeitliche Diskrepanz zwischen dem Anstieg der mRNA-Level und der Proteinexpression. Wir führen dies auf die komplex regulierten Translationsprozesse (Ingolia, Lareau and Weissman, 2011) und posttranslationale Modifikationen (Ramazi and Zahiri, 2021) zurück.

Eine wichtige Erkenntnis der vorliegenden Studie ist, dass trotz ähnlicher semiologischer Ausprägung der beider experimenteller TLEs (Curia *et al.*, 2008; Pitsch *et al.*, 2012b, 2017; Bedner *et al.*, 2015) möglicherweise verschiedene zugrundeliegende Pathomechanismen eine Rolle spielen, die unterschiedliche zeitliche Verläufe der Entzündungsaktivität verursachen. Die Ergebnisse im KA-Modell weisen auf zwei Phasen der Entzündungsreaktion im Hippocampus hin: eine akute Phase als Reaktion auf Exzitotoxizität und Status epilepticus (SE) und eine chronische Phase, die von anhaltender Entzündung und Zellumbau geprägt ist und schließlich zur Zerstörung des Hippocampus führt. Letzteres könnte durch einen sich selbst aufrechterhaltenden Entzündungszyklus wie den NLRP3-Signalweg verursacht werden.

Zusammenfassend legen unsere Daten nahe, dass die Aktivierung des Inflammasom-Signalwegs und die Anfallsaktivität miteinander verbunden sind und untrennbar mit dem chronischen epileptischen Zustand einhergehen. Da die Transkriptomprofile der Epilepsie dynamisch sind und von verschiedenen Faktoren abhängen, sind weitere Untersuchungen erforderlich, um spezifische molekulare Komponenten der Inflammasom-Signalübertragung zu identifizieren, die für pharmakoresistente TLE von Bedeutung sind. Nur durch ein besseres Verständnis der pathogenetischen Grundlagen dieser Erkrankung können wir gezielte Therapien für diese schwer behandelbare Erkrankung entwickeln.

1.5 Zusammenfassung

Ziel dieser Arbeit ist es, den Zusammenhang zwischen der Aktivierung des NLRP3-Signalwegs und der Epileptogenese näher aufzuschlüsseln. Die mRNA-Expression von NLRP3 und assoziierten Signalmolekülen im Hippocampus wurde in zwei post-SE-Mausmodellen für pharmakoresistente TLE, dem systemischen Pilocarpin- und dem suprahippocampalen KA-Modell, longitudinal analysiert. Zusätzlich wurden

immunhistochemische Untersuchungen durchgeführt, um die Einwanderung und Aktivierung von Mikroglia und Astrozyten zu untersuchen. An humanem Hippocampus-Biopsiegewebe von Patienten mit Hippocampussklerose (n=78) im Vergleich zu Patienten mit läsionsassoziierter chronischer TLE (n=34) wurden Genexpressionsanalysen der NLRP3-Signalkasade durchgeführt.

Die humanen Genexpressionsanalysen in Gehirngewebe von Patienten mit HS- oder mit läsionsassoziierter TLE zeigte, dass die Expression NLRP3-assoziierter Moleküle weitestgehend unabhängig vom Maß des neuronalen Zellverlusts und der strukturellen Reorganisation des Hippocampus ist.

In beiden murinen Epilepsiemodellen waren sämtliche Schlüsselkomponenten des NLRP3-Signalwegs auf mRNA-Ebene signifikant erhöht. Der zeitliche Verlauf der proinflammatorischen mRNA-Expressionsänderungen war jedoch modellabhängig verschieden. Pilocarpin-induzierter SE führte zu einer Zunahme der NLRP3-assoziierten Signalmoleküle hauptsächlich während der frühen Epileptogenese bis zehn Tage nach SE-Induktion. Im Gegensatz dazu erreichten Tiere mit KA-induziertem SE die höchsten mRNA-Werte in der chronischen Phase. Die Einwanderung und Aktivierung von Mikroglia und Astrozyten folgte einem ähnlichen, modellabhängigen Zeitverlauf.

Diese Studie untersucht die NLRP3-assoziierte Neuroinflammation über eine große Zeitspanne nach induziertem SE und weist eine starke Aktivierung des NLRP3-Signalwegs in den zwei häufig verwendeten post-SE-Modellen der TLE auf. Obwohl man davon ausgeht, dass die Pathogenese der TLE in beiden Modellen recht ähnlich ist, wurden deutliche Unterschiede im zeitlichen Verlauf der Anfallsentwicklung, des neuronalen Zelltods und der molekularen Reorganisation festgestellt. Die genaue Kenntnis der spezifischen Merkmale jedes Tiermodells ermöglicht es uns, die der Epilepsie zugrundeliegenden Mechanismen zu analysieren, um Angriffspunkte für maßgeschneiderte Therapieoptionen zu finden.

1.6 Literaturverzeichnis

Asadi-Pooya AA, Stewart GR, Abrams DJ and Sharan A. Prevalence and Incidence of Drug-Resistant Mesial Temporal Lobe Epilepsy in the United States. World Neurosurg. 2017. 99: 662–666

Bauer J, Becker AJ, Elyaman W, Peltola J, Rüegg S, Titulaer MJ, Varley JA and Beghi E. Innate and adaptive immunity in human epilepsies. Epilepsia. 2017. 58: 57–68

Bauernfeind FG, Horvath G, Stutz A, Alnemri ES, MacDonald K, Speert D, Fernandes-Alnemri T, Wu J, Monks BG, Fitzgerald KA, Hornung V and Latz E. Cutting Edge: NF-κB Activating Pattern Recognition and Cytokine Receptors License NLRP3 Inflammasome Activation by Regulating NLRP3 Expression. J. Immunol. 2009. 183: 787–791

Becker AJ, Chen J, Zien A, Sochivko D, Normann S, Schramm J, Elger CE, Wiestier OD and Blümcke I. Correlated stage- and subfield-associated hippocampal gene expression patterns in experimental and human temporal lobe epilepsy. Eur. J. Neurosci. 2003. 18: 2792–2802

Becker AJ, Pitsch J, Sochivko D, Opitz T, Staniek M, Chen C-C, Campbell KP, Schoch S, Yaari Y and Beck H. Transcriptional Upregulation of Ca v 3.2 Mediates Epileptogenesis in the Pilocarpine Model of Epilepsy. J. Neurosci. 2008. 28: 13341–13353

Becker AJ. Review: Animal models of acquired epilepsy: insights into mechanisms of human epileptogenesis. Neuropathol. Appl. Neurobiol. 2018. 44: 112–129

Bedner P, Dupper A, Hüttmann K, Müller J, Herde MK, Dublin P, Deshpande T, Schramm J, Häussler U, Haas CA, Henneberger C, Theis M and Steinhäuser C. Astrocyte uncoupling as a cause of human temporal lobe epilepsy. Brain. 2015. 138: 1208–1222

Bergsbaken T, Fink SL, den Hartigh AB, Loomis WP and Cookson BT. Coordinated Host Responses during Pyroptosis: Caspase-1–Dependent Lysosome Exocytosis and Inflammatory Cytokine Maturation. J. Immunol. 2011. 187: 2748–2754

Blümcke I, Pauli E, Clusmann H, Schramm J, Becker A, Elger C, Merschhemke M, Meencke HJ, Lehmann T, Von Deimling A, Scheiwe C, Zentner J, Volk B, Romstöck J, Stefan H and Hildebrandt M. A new clinico-pathological classification system for mesial

temporal sclerosis. Acta Neuropathol. 2007. 113: 235–244

Blümcke I et al. International consensus classification of hippocampal sclerosis in temporal lobe epilepsy: A Task Force report from the ILAE Commission on Diagnostic Methods. Epilepsia. 2013. 54: 1315–1329

Covolan L and Mello LEAM. Temporal profile of neuronal injury following pilocarpine or kainic acid-induced status epilepticus. Epilepsy Res. 2000. 39: 133–152

Crespel A, Coubes P, Rousset M-C, Brana C, Rougier A, Rondouin G, Bockaert J, Baldy-Moulinier M and Lerner-Natoli M. Inflammatory reactions in human medial temporal lobe epilepsy with hippocampal sclerosis. Brain Res. 2002. 952: 159–69

Cristina de Brito Toscano E, Leandro Marciano Vieira É, Boni Rocha Dias B, Vidigal Caliari M, Paula Gonçalves A, Varela Giannetti A, Maurício Siqueira J, Kimie Suemoto C, Elaine Paraizo Leite R, Nitrini R, Alvarenga Rachid M and Lúcio Teixeira A. NLRP3 and NLRP1 inflammasomes are up-regulated in patients with mesial temporal lobe epilepsy and may contribute to overexpression of caspase-1 and IL-β in sclerotic hippocampi. Brain Res. 2021. 1752: 147230

Curia G, Longo D, Biagini G, Jones RSG and Avoli M. The pilocarpine model of temporal lobe epilepsy. J. Neurosci. Methods. 2008. 143–157

Ingolia NT, Lareau LF and Weissman JS. Ribosome profiling of mouse embryonic stem cells reveals the complexity and dynamics of mammalian proteomes. Cell. 2011. 147: 789–802

Iori V, Iyer AM, Ravizza T, Beltrame L, Paracchini L, Marchini S, Cerovic M, Hill C, Ferrari M, Zucchetti M, Molteni M, Rossetti C, Brambilla R, Steve White H, D'Incalci M, Aronica E and Vezzani A. Blockade of the IL-1R1/TLR4 pathway mediates disease-modification therapeutic effects in a model of acquired epilepsy. Neurobiol. Dis. 2017. 99: 12–23

Jiang J, Yang M soon, Quan Y, Gueorguieva P, Ganesh T and Dingledine R. Therapeutic window for cyclooxygenase-2 related anti-inflammatory therapy after status epilepticus. Neurobiol. Dis. 2015. 76: 126–136

Johnson AM, Sugo E, Barreto D, Hiew C-C, Lawson JA, Connolly AM, Somerville E, Hasic E, Bye AM and Cunningham AM. The Severity of Gliosis in Hippocampal Sclerosis Correlates with Pre-Operative Seizure Burden and Outcome After Temporal

Lobectomy. Mol. Neurobiol. 2016. 53: 5446–56

Kral T, Clusmann H, Urbach J, Schramm J, Elger C, Kurthen M and Grunwald T. Preoperative evaluation for epilepsy surgery (Bonn Algorithm). Zentralbl. Neurochir. 2002. 63: 106–110

Leal B, Chaves J, Carvalho C, Rangel R, Santos A, Bettencourt A, Lopes J, Ramalheira J, Silva BM, da Silva AM and Costa PP. Brain expression of inflammatory mediators in Mesial Temporal Lobe Epilepsy patients. J. Neuroimmunol. 2017. 313: 82–88

Van Loo KMJ, Schaub C, Pitsch J, Kulbida R, Opitz T, Ekstein D, Dalal A, Urbach H, Beck H, Yaari Y, Schoch S and Becker AJ. Zinc regulates a key transcriptional pathway for epileptogenesis via metal-regulatory transcription factor 1. Nat. Commun. 2015. 6: 8688

Maroso M, Balosso S, Ravizza T, Liu J, Aronica E, Iyer A, Rossetti C, Molteni M, Casalgrandi M, Manfredi A, Bianchi M and Vezzani A. Toll-like receptor 4 and high-mobility group box-1 are involved in ictogenesis and can be targeted to reduce seizures. Nat. Med. 2010. 16: 413–419

Maroso M, Balosso S, Ravizza T, Iori V, Wright CI, French J and Vezzani A. Interleukin-1β Biosynthesis Inhibition Reduces Acute Seizures and Drug Resistant Chronic Epileptic Activity in Mice. Neurotherapeutics. 2011. 8: 304–315

Mello LEAM, Cavalheiro EA, Tan AM, Kupfer WR, Pretorius JK, Babb TL and Finch DM. Circuit mechanisms of seizures in the pilocarpine model of chronic epilepsy: cell loss and mossy fiber sprouting. Epilepsia. 1993. 34: 985–995

Meng XF, Tan L, Tan MS, Jiang T, Tan CC, Li MM, Wang HF and Yu JT. Inhibition of the NLRP3 inflammasome provides neuroprotection in rats following amygdala kindling-induced status epilepticus. J. Neuroinflammation. 2014. 11: 212

Pernhorst K, Herms S, Hoffmann P, Cichon S, Schulz H, Sander T, Schoch S, Becker AJ and Grote A. TLR4, ATF-3 and IL8 inflammation mediator expression correlates with seizure frequency in human epileptic brain tissue. Seizure. 2013. 22: 675–678

Pitsch J, Schoch S, Gueler N, Flor PJ, van der Putten H and Becker AJ. Functional role of mGluR1 and mGluR4 in pilocarpine-induced temporal lobe epilepsy. Neurobiol. Dis. 2007. 26: 623–633

Pitsch J, Opitz T, Borm V, Woitecki A, Staniek M, Beck H, Becker AJ and Schoch S. The presynaptic active zone protein rim α controls epileptogenesis following status epilepticus. J. Neurosci. 2012a. 32: 12384–12395

Pitsch J, Opitz T, Borm V, Woitecki A, Staniek M, Beck H, Becker AJ and Schoch S. The presynaptic active zone protein rim α controls epileptogenesis following status epilepticus. J. Neurosci. 2012b. 32: 12384–12395

Pitsch J, Becker AJ, Schoch S, Müller JA, de Curtis M and Gnatkovsky V. Circadian clustering of spontaneous epileptic seizures emerges after pilocarpine-induced status epilepticus. Epilepsia. 2017. 58: 1159–1171

Pitsch J, Kuehn JC, Gnatkovsky V, Müller JA, van Loo KMJJ, de Curtis M, Vatter H, Schoch S, Elger CE and Becker AJ. Anti-epileptogenic and Anti-convulsive Effects of Fingolimod in Experimental Temporal Lobe Epilepsy. Mol. Neurobiol. 2019. 56: 1825–1840

Ramazi S and Zahiri J. Post-translational modifications in proteins: Resources, tools and prediction methods. Database. [Preprint] 2021.

Ravizza T, Gagliardi B, Noé F, Boer K, Aronica E and Vezzani A. Innate and adaptive immunity during epileptogenesis and spontaneous seizures: evidence from experimental models and human temporal lobe epilepsy. Neurobiol. Dis. 2008. 29: 142–60

Rizzi M, Perego C, Aliprandi M, Richichi C, Ravizza T, Colella D, Velískŏvá J, Moshé SL, De Simoni MG and Vezzani A. Glia activation and cytokine increase in rat hippocampus by kainic acid-induced status epilepticus during postnatal development. Neurobiol. Dis. 2003. 14: 494–503

Schroder K and Tschopp J. The Inflammasomes. Cell. 2010. 140: 821–832

Vakharia VN, Duncan JS, Witt JA, Elger CE, Staba R and Engel J. Getting the best outcomes from epilepsy surgery. Ann. Neurol. 2018. 676–690

Vezzani A, Moneta D, Conti M, Richichi C, Ravizza T, De Luigi A, De Simoni MG, Sperk G, Andell-Jonsson S, Lundkvist J, Iverfeldt K and Bartfai T. Powerful anticonvulsant action of IL-1 receptor antagonist on intracerebral injection and astrocytic overexpression in mice. Proc. Natl. Acad. Sci. U. S. A. 2000. 97: 11534–9

Vezzani A, Moneta D, Richichi C, Aliprandi M, Burrows SJ, Ravizza T, Perego C and Grazia De Simoni M. Functional role of inflammatory cytokines and antiinflammatory molecules in seizures and epileptogenesis. Epilepsia. 2002. 43: 30–35

Vezzani A, Balosso S and Ravizza T. The role of cytokines in the pathophysiology of epilepsy. Brain. Behav. Immun. 2008. 22: 797–803

Vezzani A and Rüegg S. The pivotal role of immunity and inflammatory processes in epilepsy is increasingly recognized: introduction. Epilepsia. 2011. 52 Suppl 3: 1–4

Vezzani A and Viviani B. Neuromodulatory properties of inflammatory cytokines and their impact on neuronal excitability. Neuropharmacology. 2015. 96: 70–82

Wu C, Zhang G, Chen L, Kim S, Yu J, Hu G, Chen J, Huang Y, Zheng G and Huang S. The Role of NLRP3 and IL-1β in Refractory Epilepsy Brain Injury. Front. Neurol. 2020. 10: 1–8

Yue J, Wei YJ, Yang XL, Liu SY, Yang H and Zhang CQ. NLRP3 inflammasome and endoplasmic reticulum stress in the epileptogenic zone in temporal lobe epilepsy: molecular insights into their interdependence. Neuropathol. Appl. Neurobiol. 2020. 46: 779–785

Zhao X, Liao Y, Morgan S, Gruenthal M, Zhao X, Liao Y, Morgan S, Mathur R, Feustel P, Mazurkiewicz J and Qian J. Noninflammatory Changes of Microglia Are Sufficient to Cause Epilepsy. CellReports. 2018. 22: 2080–2093

3. Veröffentlichung

PLOS ONE

RESEARCH ARTICLE

Characterisation of NLRP3 pathway-related neuroinflammation in temporal lobe epilepsy

Malin S. Pohlentz[1], Philipp Müller[1], Silvia Cases-Cunillera[1], Thoralf Opitz[2], Rainer Surges[3,4], Motaz Hamed[5], Hartmut Vatter[5], Susanne Schoch[1,3], Albert J. Becker[1☯], Julika Pitsch[1,3☯*]

1 Dept. of Neuropathology, Section for Translational Epilepsy Research, University Hospital Bonn, Bonn, Germany, **2** Inst. for Experimental Epileptology and Cognition Research, University Hospital Bonn, Bonn, Germany, **3** Dept. of Epileptology, University Hospital Bonn, Bonn, Germany, **4** Center for Rare Diseases Bonn (ZSEB), University Hospital Bonn, Bonn, Germany, **5** Dept. of Neurosurgery, University Hospital Bonn, Bonn, Germany

☯ These authors contributed equally to this work.
* jpitsch@uni-bonn.de

Citation: Pohlentz MS, Müller P, Cases-Cunillera S, Opitz T, Surges R, Hamed M, et al. (2022) Characterisation of NLRP3 pathway-related neuroinflammation in temporal lobe epilepsy. PLoS ONE 17(8): e0271995. https://doi.org/10.1371/journal.pone.0271995

Editor: Stephen D. Ginsberg, Nathan S Kline Institute, UNITED STATES

Received: November 4, 2021

Accepted: July 11, 2022

Published: August 16, 2022

Peer Review History: PLOS recognizes the benefits of transparency in the peer review process; therefore, we enable the publication of all of the content of peer review and author responses alongside final, published articles. The editorial history of this article is available here: https://doi.org/10.1371/journal.pone.0271995

Data Availability Statement: All relevant data are within the paper and its Supporting Information files.

Abstract

Objective

Inflammation of brain structures, in particular the hippocampal formation, can induce neuronal degeneration and be associated with increased excitability manifesting as propensity for repetitive seizures. An increase in the abundance of individual proinflammatory molecules including interleukin 1 beta has been observed in brain tissue samples of patients with pharmacoresistant temporal lobe epilepsy (TLE) and corresponding animal models. The NLRP3-inflammasome, a cytosolic protein complex, acts as a key regulator in proinflammatory innate immune signalling. Upon activation, it leads to the release of interleukin 1 beta and inflammation-mediated neurodegeneration. Transient brain insults, like status epilepticus (SE), can render hippocampi chronically hyperexcitable and induce segmental neurodegeneration. The underlying mechanisms are referred to as epileptogenesis. Here, we have tested the hypothesis that distinct NLRP3-dependent transcript and protein signalling dynamics are induced by SE and whether they differ between two classical SE models. We further correlated the association of NLRP3-related transcript abundance with convulsive activity in human TLE hippocampi of patients with and without associated neurodegenerative damage.

Methods

Hippocampal mRNA- and protein-expression of NLRP3 and associated signalling molecules were analysed longitudinally in pilocarpine- and kainic acid-induced SE TLE mouse models. Complementarily, we studied NLRP3 inflammasome-associated transcript patterns in epileptogenic hippocampi with different damage patterns of pharmacoresistant TLE patients that had undergone epilepsy surgery for seizure relief.

Funding: Our work is supported by the Deutsche Forschungsgemeinschaft (to AJB: SFB 1089; to SS: SCHO 820/4-1, SCHO 820/6-1, SCHO 820/7-1, SCHO 820/5-2, SPP1757, SFB1089; to AJB: FOR 2715), Else Kröner-Fresenius-Foundation (Promotionskolleg 'NeuroImmunology' to MP, SS, AJB; 2016_A05 to JP), as well as the BONFOR program of the Medical Faculty, University of Bonn (MP, SS, AJB, JP). The funders had no role in study design, data collection and analysis, decision to publish, or preparation of the manuscript. There was no additional external funding received for this study.

Competing interests: The authors have declared that no competing interests exist.

Results

Pilocarpine- and kainic acid-induced SE elicit distinct hippocampal *Nlrp3*-associated molecular signalling. Transcriptional activation of NLRP3 pathway elements is associated with seizure activity but independent of the particular neuronal damage phenotype in KA-induced and in human TLE hippocampi.

Significance

These data suggest highly dynamic inflammasome signalling in SE-induced TLE and highlight a vicious cycle associated with seizure activity. Our results provide promising perspectives for the inflammasome signalling pathway as a target for anti-epileptogenic and -convulsive therapeutic strategies. The latter may even applicable to a particularly broad spectrum of TLE patients with currently pharmacoresistant disease.

Introduction

Temporal lobe epilepsy (TLE) is the most frequent form of focal epilepsy in adults [1] and is often triggered by a transient brain insult or injury. A cascade of molecular, cellular and physiological alterations results in the evolution of chronic recurrent seizures. This development of an epileptic condition and/or the progression of epilepsy after its establishment is referred to as 'epileptogenesis' [2] but the underlying mechanisms have remained unresolved. A better understanding of the pathogenesis is urgently needed, as a fraction of TLE patient does not respond to antiseizure drugs [1]. Surgical removal of the epileptogenic focus can potentially decrease or even abolish seizures in many patients suffering from drug-refractory TLE [3]. The most frequent neuropathological finding in resected tissue of these individuals is hippocampal sclerosis (HS) [3], which is characterised by segmental neuronal cell loss, microgliosis and reactive astrogliosis [4, 5]. This lesion pattern in concert with the development of chronic recurrent seizures is reproduced in Status epilepticus (SE) induced TLE mouse models [6] induced either by the excitotoxic compounds pilocarpine [7] or kainic acid (KA) [8, 9].

Recent data point to an important role of aseptic inflammatory signalling in the development and maintenance of TLE [10, 11]. Blockade of pro-inflammatory signalling molecules represents a promising approach for a disease-modifying treatment of TLE [12–15]. An example of an important key regulator responsible for the release of proinflammatory cytokines is the NOD-like receptor protein 3 (NLRP3). Upon toll-like receptor 4 (TLR4) activation, downstream signalling leads to Nuclear Factor κB (NFκB) dependent expression of both pro-interleukin-1-beta (*pro-Il1b*) and *Nlrp3* mRNA [16]. After transcriptional upregulation, a second danger signal leads to the formation of the NLRP3 inflammasome [17], which comprises NLRP3, apoptosis-associated speck-like protein (ASC) and pro-caspase-1. The inflammasome then cleaves pro-caspase-1, which promotes Interleukin 1 beta (IL1B) activation and release [18].

Inhibition of individual components of the NLRP3 pathway attenuates neuroinflammation and reduces seizure frequency and severity in experimental TLE [12, 15, 19–21]. Molecules involved in NLRP3 signalling have been detected in HS-TLE, in which the hippocampus shows extensive neuronal damage [12, 22–25]. si-RNA mediated knockdown of *Nlrp3* acted neuroprotectively and also attenuated the chronic seizure phenotype in an electrically induced SE model in rats [13]. *NLRP3* knockout reduced neuronal necrosis and apoptosis as well as peripheral blood levels of IL1B one week after pilocarpine-induced SE in mice [12].

SE-induced TLE models have different structural and functional characteristics dependent on the excitotoxic compound (for review see [26]). Here, we have examined, which hippocampal inflammasome-related molecular dynamics emerge from systemic pilocarpine- versus unilaterally suprahippocampal KA-induced SE. Additionally, we investigated whether the extent of neuronal damage affects transcriptional changes of inflammasome-related molecules. In a translational effort, we have further tested, whether differential inflammasome-related molecular signatures occur in chronic TLE hippocampi with epileptogenesis and extensive neuronal damage versus hippocampi from lesion-associated TLE. The latter are characterized by a general lack of epileptogenesis and HS, despite being chronically epileptic. Our results suggest robust and sustained activation of inflammasome-mediated signalling in experimental and human TLE hippocampi independent of a specific damage pattern.

Methods

Animals

All animal procedures were planned and performed to minimize pain and suffering and to reduce the number of used animals in accordance with the guidelines of the University Hospital Bonn, Animal-Care-Committee as well as the guidelines approved by the European Directive (2010/63/EU) on the protection of animals used for experimental purposes and ARRIVE guidelines. All mice were housed in a humidity (55 ± 10%) and temperature (22 ± 2˚C) controlled environment under a 12-h light–dark-cycle (light cycle 7 am to 7 pm) with water and food ad libitum and nesting material (Nestlets, Ancare, USA). Mice were allowed to adapt to the animal facility at least for seven days before any treatment.

Induction of chronic epilepsy by suprahippocampal kainic acid injection

As described previously, anaesthetized [16 mg/kg xylazine (Ceva Tiergesundheit, Germany) and 100 mg/kg ketamine, i.p. (Ketamin 10%, WDT, Germany)] male C57Bl6/N mice (Charles River; ~60 days old, weight $\geq$ 20 g) were used for induction of chronic epilepsy. Briefly, 70 nl kainic acid (20 mM in 0.9% NaCl, Tocris) was applied over 2 min unilaterally above the CA1 region of the left dorsal hippocampus (stereotaxic coordinates in mm relative to Bregma: -2 anterioposterior, -1.5 mediolateral, and -1.4 dorsoventral) using a Nanofil syringe (WPI) operated by a micropump (WPI) [27]. Control (non-SE) mice were injected in the same manner with 70 nl 0.9% NaCl. After injection the syringe was left for additional 2 min to avoid reflux. All operated mice received analgesic treatment before and once per day for 3 days post-surgery (5 mg/kg Ketoprofen, s.c.; Gabrilen, mibe). With this method the incidence of inducing SE is 100% without any mortality [27]. All animals exhibit chronic behavioural focal to bilateral tonic-clonic seizures (10d, 28d group).

Induction of chronic epilepsy by systemic pilocarpine injection

To induce SE, animals (male C57Bl6/N mice; Charles River; ~60 days old, weight $\geq$ 20 g) were injected subcutaneously with 335 mg/kg pilocarpine hydrochloride (Sigma), 20 min after pretreatment with subcutaneous injection of 1 mg/kg scopolamine methyl nitrate (Sigma) as described in previous publications [28, 29]. Forty min after SE onset, animals received an injection of diazepam (4 mg/kg, s.c.; Ratiopharm). Control (non-SE) animals were treated identically but received saline instead of pilocarpine. Behavioural SE was clearly identified using a modified seizure scheme sustained continuous convulsions with postural loss designated as SE [28, 29]. Among pilocarpine injected animals, only those that developed SE (SE-

experienced) were further used for analysis. All SE-experienced animals showed behavioural focal to bilateral tonic-clonic seizures at later model stages (5d, 10d, 28d group).

Telemetric video/EEG monitoring

Semiological aspects of were analysed in male C57Bl6/N mice (Charles River; ~60 days old, weight $\geq$ 20 g) for 28 days after KA- or pilocarpine-induced SE by using 24/7 telemetric EEG/video monitoring. EEG implantation, postoperative treatment, continuous telemetric EEG-/video-monitoring, and behavioral seizure classification were previously described in detail [27, 29]. Two weeks before pilocarpine injection or directly after KA injection, a cortical ECoG electrode was implanted (in mm relative to Bregma: -2 AP, -1.5 ML) with subcutaneously placed transmitters (ETA-F20, DSI). A stainless-steel screw in contact with the cerebellar cortex of the simple lobe at the midline (in mm relative to Bregma: -6 AP, 0 ML, 0 DV) was used to fix the reference electrode. Appropriate placement of the electrodes was assessed histologically in all mice at the end of the experiment. Continuous EEG recording with a sampling rate of 1 kHz was started directly after electrode implantation and performed and analysed using NeuroScore v3.2 (DSI) software. From concurrent video recordings, seizures were classified as described before [27, 29].

Murine mRNA isolation, real-time RT-PCR quantification, histopathological analysis, cell quantification

mRNA was isolated from microdissected hippocampal CA1 region at different time points after induced SE using magnetic beads (mRNA Direct™ Micro Kit, Invitrogen) followed by cDNA synthesis (RevertAid H Minus First Strand cDNA Synthesis Kit, Thermo Scientific) as described before [27]. Briefly, transcripts of different genes were quantified by RT-PCR using CFX384 Touch Real-Time PCR Detection System (Biorad) and determined with the $\Delta\Delta C_t$ method. PCR samples for quantification of ASC and NFκB2 contained 3 μl Maxima Probe/ROX qPCR Master Mix (2x) (Thermo Scientific), 0.3 μl of TaqMan™ Gene Expression Assay (Thermo Scientific, Mm00479807_m1, Hs01547324_gH), 1.7 μl RNase free water and 2 μl cDNA. All other PCR samples contained 3.125 μl Maxima SYBR Green/ROX qPCR Master Mix (2x) (Thermo Scientific, K0223), 0.3 μM of each oligonucleotide primer (*Nlrp3*: FW: AATGCCCTTGGAGACACAGG and RV: ATTCCAGCAGCTGTGTGAGG; *Casp1*: FW: GGACCCTCAAGTTTTGCCGCT and RV: ATGAGGGCAAGACGTGTACG; *Aif1*: FW: TCAGAATGATGCTGGGCAAG and RV: GACCAGTTGGCCTCTTGTGT; *Gfap*: FW: AGAAAACCGCATCACCATTC and RV: TCTTGAGGTGGCCTTCTGAC; *Il1b*: FW: CACTACAGGCTCCGAGATGA and RV: TTTGTCGTTGCTTGGTTCTC; TLR4: FW: CCAATTTTTCAGAACTTCAGTGG and RV: AGAGGTGGTGTAAGCCATGC; *β-actin*: FW: ACCGTGAAAAGATGACCCAGA and RV: ATGGGCACAGTGTGGGTGA), 1.5 μl cDNA and 1.5 μl of RNase free water. RT-PCR was performed using the following steps: 2 min at 50˚C, 10 min at 95˚C, then 40 cycles of 15 s at 95˚C, 30 s at 60˚C and 30 s at 72˚C. For KA-injected animals, the data of left and right CA1 region were pooled because no significant differences were found between both hemispheres (**S1A Fig**).

For immunohistochemistry, mice were decapitated under isoflurane anaesthesia (Forene®, Abbott, Germany). Brains were removed quickly, fixed in 4% PFA overnight and embedded in paraffin. Coronal sections (4 μm thick) were used for GFAP (glial fibrillary protein; to label reactive astrogliosis, NeuroMab, 1:250), NeuN (Neuronal nuclei; to label neuronal somata, Millipore, 1:500), AIF1 (allograft inflammatory factor 1; to label activated microglia, Wako, 1:1000), IL1B (Interleukin 1 beta, abcam, 1:100) as described previously [27]. Briefly, paraffin sections were deparaffinized and washed in distilled water. Antigen retrieval mediated by citric acid (10mM, pH 6,0) was performed at 90˚C for 8 min. After washing, brain sections were

blocked for 2 h at 37˚C in PBS buffer containing 10% normal goat serum, 1% fetal calf serum, and incubated with primary antibodies over night at 4˚C. After washing, slides were incubated with respective secondary antibodies (Life technologies, 1:100) and DAPI (4′,6-Diamidino-2-phenylindole dihydrochloride, Sigma, 1:100.000) in blocking buffer, washed and mounted with Mowiol 4–88 (Roth).

For semi-quantitative analysis of microglia and astrocytes, DAB (3,3′-Diamino-benzidin) staining was used. After blocking with 5% normal goat serum diluted in PBS for 1 h at 37˚C, slices were washed and incubated with GFAP (Sigma, 1:500) and AIF1 (Wako, 1:1000) overnight at 4˚C. After washing, slices were incubated with respective biotinylated secondary antibodies (Vector Laboratories, USA, 1:200) in blocking buffer and incubated for 2 h at 37˚C. Slides were again washed and further processed according to manufacturer's protocol (Sigmafast, Merck, Germany) and mounted with Mowiol 4–88 (Roth).

All non-fluorescent digital images were captured with a microscope (BZ-X, Keyence, Japan) and fluorescent images with a confocal microscope (Nikon, Eclipse T*i*). For cell quantification, Fiji (ImageJ) software was used to apply colour deconvolution to change RGB images to DAB and a global threshold was applied to the DAB channel to get a binary image. The resultant data was extracted as area fraction (ranging from 0 to 100). Three sections from each mouse (between -1.6 mm and -2.1 mm anterio-posterior relative to Bregma) and within each section, three adjacent fields of CA1 were quantified.

Human TLE patients, mRNA sequencing and histopathological analysis

Gene expression analyses were applied on human hippocampal biopsy tissue from patients with hippocampal sclerosis (n = 78) versus patients with lesion-associated chronic TLE (involving low-grade neoplasms / dysplasia; n = 34), who underwent surgical treatment in the Epilepsy Surgery Program at the University Hospital Bonn due to pharmacoresistance [30]. The general clinical data are now summarized in **S1 Table**. In all patients, presurgical evaluation using a combination of non-invasive and invasive procedures revealed that seizures originated in the mesial temporal lobe [31]. For each case included in the present study, hippocampal tissue samples were available for neuropathologic examination. The HS group was clearly characterized by segmental neuronal cell loss and concomitant astrogliosis and microglial activation. The hippocampi in the control group showed no segmental neuronal cell loss neuropathologically but exhibited astrogliosis and microglial activation and were therefore consistent with lesions such as cortical dysplasia or epilepsy-associated tumors. In each case, the diagnosis was made by an experienced neuropathologist (AJB) according to international criteria [32, 33]. All procedures were conducted in accordance with the Declaration of Helsinki and approved by the Ethics Committee of the University Hospital Bonn (222/16). Informed written consent was obtained from all patients. mRNA analyses for *Nlrp3*, *Casp1*, *Tlr4*, *NfkB2*, *Il1b*, *Il18*, *Gfap* and *Aif1* were carried out analogous to a procedure described elsewhere in detail [34]. Briefly, RNA from hippocampal biopsies served to generate 750 ng cRNA used for hybridization on Human HT-12 v3 Expression BeadChips with Illumina Direct Hybridization Assay Kit (Illumina, San Diego, CA) according to standard procedures. We extracted data for our genes of interest analysed by Illumina's GenomeStudio Gene Expression Module and normalized using Illumina BeadStudio software suite by quantile normalization with background subtraction.

For histological analysis, human surgical brain tissue was fixed with formaldehyde overnight, embedded into paraffin. 4 μm sections were used for both, hematoxylin-eosin (H&E) staining and immunohistochemistry by using standard protocols [35]. Briefly, paraffin sections were de-paraffinized in xylene for 10 min followed by decreasing alcohol series (100–

50%) for 2 min each. After washing, slides were subjected to a citric acid antigen retrieval procedure, followed by two washing steps. Subsequently, brain sections were rinsed for 2 h at 37˚C in PBS blocking buffer (10% normal goat serum), and incubated overnight at RT with antibodies against glial fibrillary acidic protein (GFAP, Z0334, Dako, 1:100), neuronal nuclei (NeuN, MAB377, Milipore, 1:1000), AIF1 (Wako, 1:1000), or NLRP3 (abcam, ab214185, 1:100) in PBS-blocking buffer. DAB (3,3′-Diamino-benzidin) staining was done as on murine slices (see section above). For fluorescent-immunohistochemistry, after washing slides were incubated with secondary antibody (Alexa Fluor®568, Life technologies, Germany, 1:200) and DAPI (1:100.000, Sigma, Germany) and mounted with Mowiol 4–88 (Roth, Germany). The NLRP expression pattern was evaluated by using morphological analysis.

Statistical analysis

Experiments were conducted in a randomized and blinded fashion. Prism 9 software (GraphPad Software) was used for statistical analysis. Sample size (n) per experiment was calculated using power analysis, with parameters set within the accuracy of the respective experiment. To analyse the impact of SE on the expression level of NLRP-related genes, two-way ANOVA was used with SE and time after SE being the two categorical independent variables. Sidak's multiple comparison test was used to pinpoint significant differences between control and SE group at certain time points. Mann Whitney U-test was used to analyse NLRP-related gene expression between lesion and hippocampal sclerosis sites in human specimens (for detailed statistical analysis see **S2 Table**). For correlation analysis we used the median of the summarized seizure frequency of three consecutive days before mRNA analysis for every animal (day 3: seizure sum of day 1–3; day 5: sum of day 3–5; day10: seizure sum of day 8–10; day 28: sum of day 26–28) after KA (n = 21) and pilocarpine-induced SE (n = 11). The median seizure frequency was correlated with average gene expression using simple linear regression. Statistical outliers were identified by using Grubb's test (GraphPad) and excluded from analysis. Differences between means were considered significant at $p<0.05$. All results are plotted as mean ± SD. Negative error bars crossing the x-axis limit were clipped.

Results

Transcription of NLRP3 and associated inflammasome signalling molecules is activated in a model- and time-specific manner

Transcript dynamics are important in order to trigger an inflammasome response to an insulting stimulus. Therefore, we first determined the time course of gene expression of individual molecules of the NLRP3 pathway (**Fig 1A**) during four weeks following subcutaneous pilocarpine or unilateral suprahippocampal KA injection. After pilocarpine-induced SE, *Nlrp3* expression was increased during the early stage with the highest expression after 10 days (for detailed statistical analysis see **S2 Table**). A similar pattern was observed for other inflammasome components, namely for transcripts encoding the adaptor-molecule *Asc* and the effector-molecule *Casp1*. Transcription of genes involved in the signalling cascade prior to inflammasome formation including *Tlr4* and *Nfkb2*, was also significantly augmented at 72 hours and 10 days after pilocarpine induced SE. During the later epileptic state (28 days post SE) mRNA expression was indistinguishable from control levels (**Fig 1B**). In contrast to pilocarpine-induced SE, after KA-induced SE, an increase of mRNA levels was not only observed during the early disease progression (72 hours and 5 days post SE) but also in chronic TLE stages. However, 10 days after KA-induced SE mRNA levels returned back to basal (**Fig 1C**). There

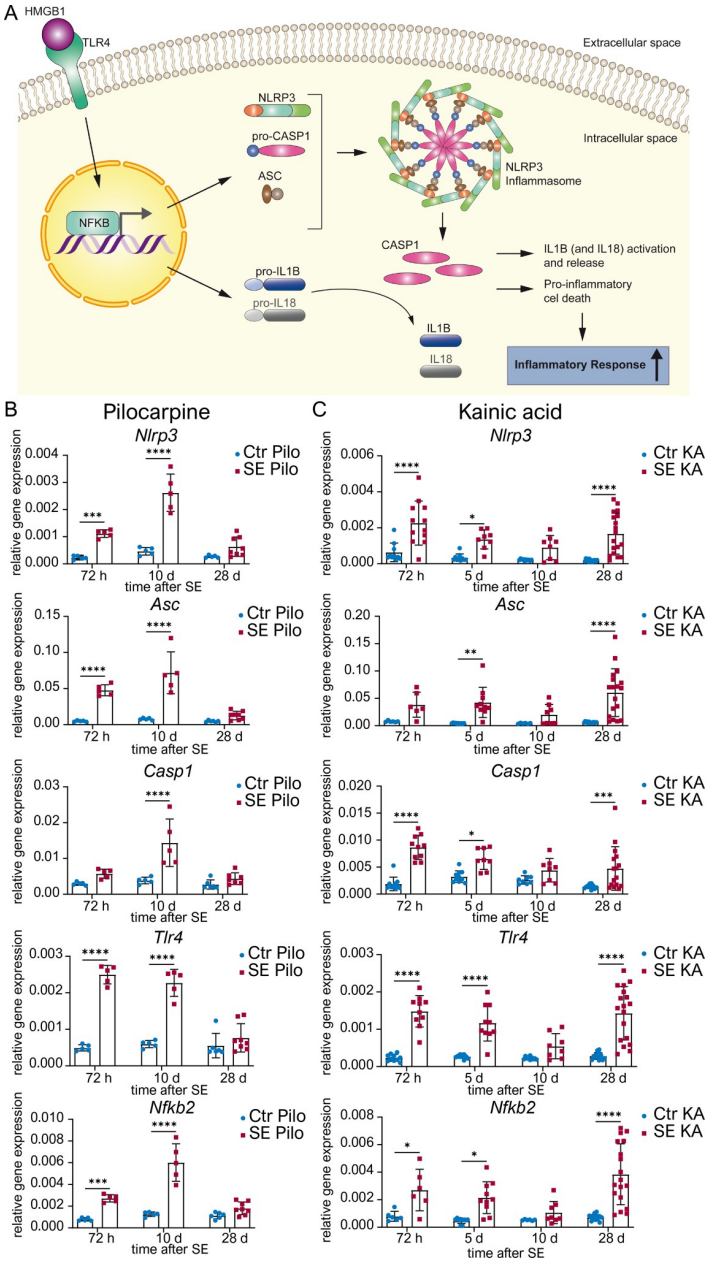

Fig 1. mRNA expression of NLRP3 and associated signalling molecules are differently regulated after SE elicited by pilocarpine or kainic acid. (**A**) Schematic representation of the NLRP3 pathway: After activation of Toll-like receptor (TLR) 4 by High-Mobility-Group-Protein (HMG) B1, nuclear factor 'kappa-light-chain-enhancer' of activated B-cells (NFKB) 2 is activated and translocates to the nucleus. Here, it enhances transcription of NOD-like receptor protein (*Nlrp*) 3 and Interleukins. Subsequently, NLRP3, Apoptosis-like-speck protein (ASC) and an inactive precursor of cysteine-dependent aspartate-specific Protease (CASP) 1 assemble to form the NLRP3 inflammasome. Upon activation of the inflammasome, pro-CASP1 is cleaved and activated, which then leads to cleavage of interleukin (IL) 1B and 18, as well as proinflammatory cell death. (**B**) Relative mRNA levels ($\Delta\Delta C_t$ method) of inflammasomal associated genes are analysed 72 h ($n \geq 5$), 10 d ($n \geq 5$) and 28 d ($n \geq 6$) after pilocarpine-induced status epilepticus (SE Pilo) as well as (**C**) 72 h ($n \geq 4$), 5 d ($n \geq 5$), 10 d ($n \geq 4$) and 28 d ($n \geq 6$) after kainic acid-induced SE in hippocampal CA1 (SE KA) compared to non-SE controls (Ctr Pilo/Ctr KA). Relative mRNA levels of NOD-like receptor protein (*Nlrp*) 3 and other inflammasomal associated genes such as *Asc*, *Casp1*, *Tlr4*, and *Nfkb2* are quantified with $\Delta\Delta C_t$ method normalized to the ubiquitously expressed (encoding proteins that are required for all cell types) housekeeping gene *β-actin* after SE. Data is shown as mean ± SD and analysed with 2way ANOVA followed by Sidak's post hoc test. Asterisks indicate significant differences between groups (control vs. SE): $^{*}p < 0.05$, $^{**}p < 0.01$, $^{***}p < 0.001$, $^{****}p < 0.0001$. Detailed statistical values are found in S2 Table.

https://doi.org/10.1371/journal.pone.0271995.g001

was no significant difference in mRNA expression level between the ipsilateral extensively damaged (KA-injected) and the contralateral side of the hippocampus (S1A Fig).

With respect to downstream effects of inflammasome activation in both experimental models, interleukin 1 mRNA and protein expression were analysed. Increased transcription of Interleukin 1 beta (*Il1b)* was only observed 10 days after pilocarpine induced SE compared to expression in the CA1 region of non-SE animals (Fig 2A**,** for detailed statistical analysis see S2 Table). In contrast, a significant decrease of Interleukin 18 (*Il18)* mRNA levels was found at 72 hours post SE (Fig 2B). A strong increase in IL1B levels was observed 72 hours after pilocarpine-induced SE in a clustered subgroup of CA1 neurons (Fig 2C). Additionally, few non-neuronal cells showed IL1B immunoreactivity. Ten days after SE, only a weak IL1B expression was detected in the remaining CA1 pyramidal neurons. However, in areas with extensive neuronal degeneration, non-neuronal cells were strongly positive for IL1B at 28 days after SE including astrocytes (Fig 2C and 2D).

In contrast, a significant increase of *Il1b* mRNA was observed at all time points investigated after KA-induced SE (Fig 3A, for detailed statistical analysis see S2 Table), whereas

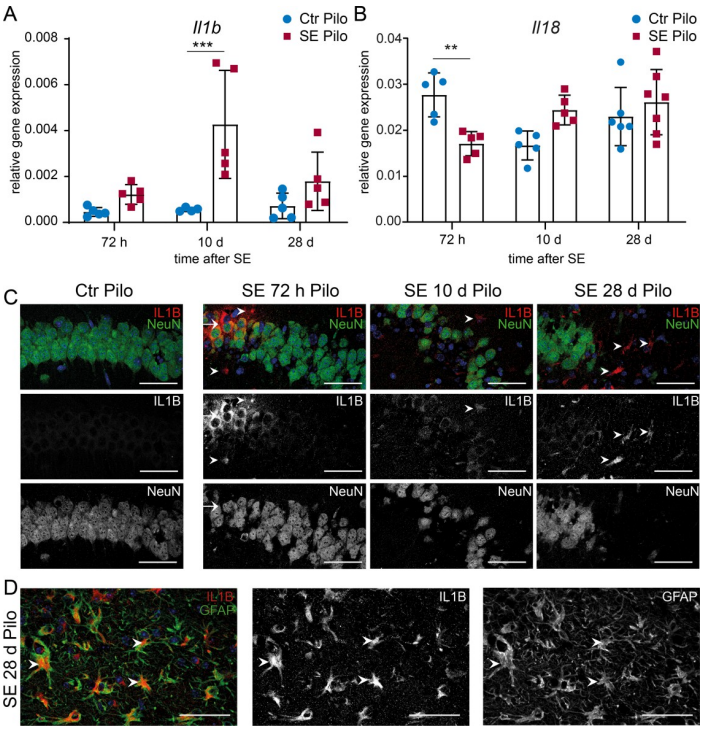

Fig 2. mRNA and protein expression levels of Interleukin 1 beta (IL1B) are transiently augmented after pilocarpine-induced SE in hippocampal CA1 region. Relative mRNA levels ($\Delta\Delta C_t$ method) of (**A**) *Il1b and* (**B**) *Il18* are analysed 72 h ($n \geq 5$), 10 d ($n \geq 5$) and 28 d ($n \geq 6$) after pilocarpine-induced SE compared to non-SE control animals (Ctr Pilo) with 2way ANOVA followed by Sidak's post hoc test. Asterisks indicate significant differences between groups (control vs. SE): $^{*}p < 0.05$, $^{**}p < 0.01$, $^{***}p < 0.001$, $^{****}p < 0.0001$. Detailed statistical values are found in S2 Table. The ubiquitously expressed *β-actin* is used as reference gene. (**C**) Representative immunohistochemistry of the hippocampal CA1 region shows 72 h after pilocarpine-induced SE a segmental expression of IL1B (red) exclusively in the CA1 pyramidal cell layer (NeuN positive neurons = green). Some non-neuronal cells are faintly IL1B positive 10 days post-SE (arrowheads). However, 28 d after SE numerous strongly IL1B positive cells are visible (arrowheads), whereas no IL1B expression is detected in non-SE control animals (leftmost, Ctrl Pilo). Scale bars: 50 μm. (**D**) A strong co-localization with GFAP within the former pyramidal cell layer indicating IL1B positive astrocytes 28 days after SE induction. Scale bars: 50 μm. 4′,6-diamidino-2-phenylindole (DAPI) for nucleic acid counterstain (blue).

https://doi.org/10.1371/journal.pone.0271995.g002

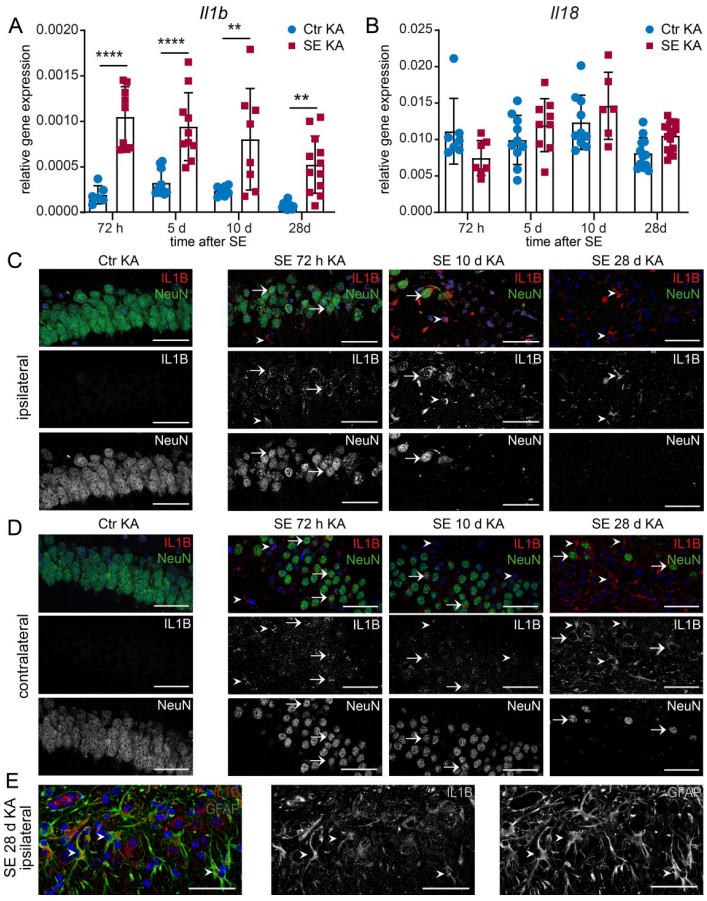

Fig 3. mRNA and protein expression levels of Interleukin 1 beta (IL1B) are augmented in the CA1 region over a period of 4 weeks after kainic acid-induced SE. (**A**) *IL1b* and (**B**) *Il18* mRNA levels ($\Delta\Delta C_t$ method) are determined 72 h ($n \geq 4$), 5 d ($n \geq 5$), 10 d ($n \geq 4$) and 28 d ($n \geq 6$) after kainic acid-induced SE compared to non-SE control animals (Ctr KA) with 2way ANOVA followed by Sidak's post hoc test. Asterisks indicate significant differences between groups (control vs. SE): $^{*}p < 0.05$, $^{**}p < 0.01$, $^{***}p < 0.001$, $^{****}p < 0.0001$. Detailed statistical values are found in S2 Table. The ubiquitously expressed *β-actin* is used as housekeeping gene. Immunohistochemistry of (**C**) ipsilateral (KA-injected) as well as (**D**) contralateral hemisphere shows single IL1B granula (red) within NeuN-postive cells (green) at 72 h post-SE (arrows). Additionally, very few non-neuronal IL1B positive cells are found (arrowheads). 10 d post-SE IL1B immunoreactivity is detected in neurons (arrows) and non-neuronal cells expressing IL1B, observed mainly in areas with vast neuronal cell loss. At 28 d post-SE, a high number of cells are IL1B positive (arrowheads) including also remaining NeuN positive cells in the contralateral hemisphere (arrows). In non-SE control animals (Ctrl KA), expression of IL1B is not detected (leftmost). Scale bars: 50 μm. DAPI for nucleic acid counterstain (blue).

https://doi.org/10.1371/journal.pone.0271995.g003

Il18 gene expression was not significantly altered in this model (Fig 3B). A granular expression of IL1B was present within neuronal somata as well as an increasing expression on non-neuronal cells at all analysed timepoints with the strongest expression after 28 days in the dorsal CA1 region (Fig 3C and 3D). Interestingly, in the chronic period, an intense IL1B expression was present on non-neuronal cells including astrocytes (Fig 3E). In addition to a large inter-individual variance in seizure frequency, the median frequency of seizure sum of three consecutive days shows minor differences between the different time points showing at both models (S3A and S3B Fig). A direct inverse correlation between seizure frequency and gene expression was observed for Interleukin 1 beta (*Il1b*) in the KA-induced model (S3B Fig **and** S2 Table).

Microglia and astrocytes exhibit different activation states during disease progression

Activated microglia and astrocytes have been shown to play an important role in neuroinflammation and activation of proinflammatory pathways in many CNS diseases including TLE [23, 36, 37]. Furthermore, astrogliosis is one of the most important hallmarks of HS. We investigated microglia and astrocytes using their specific marker proteins AIF1 and GFAP, respectively. After pilocarpine induced SE, a significant increase of *Aif1* (Fig 4A, leftmost) as well as *Gfap* (Fig 4A, rightmost) transcription was observed with real-time RT-PCR at all analysed time points. Accordingly, the area of IBA1- and GFAP-positive cells was also increasing over the observed time (Fig 4B), indicating increased cell activation. Single activated microglial cells with amoeboid shape were already present in the CA1 region 72 hours after pilocarpine-induced SE (Fig 4C). Microglial cells with a prominent cell body and little ramification accumulated along the hippocampal fissure (Fig 4C, upper panel; S2 Fig). At 10 days post-SE an increased number of microglia was observed, most prominently in the medial part of the CA1 cell band and the transition between CA1 and CA2 somata. Next to bushy morphology also various amoeboid shaped microglia (Fig 4C) were observed. Four weeks after SE, activated microglia were still present but the majority in direct proximity of CA1 pyramidal cell somata appeared more ramified (bushy) and above the hippocampal fissure with a bushy and hypertrophic shape, classified according to Wyatt-Johnson [38]. Reactive, contiguous but essentially non-overlapping astrocytes with

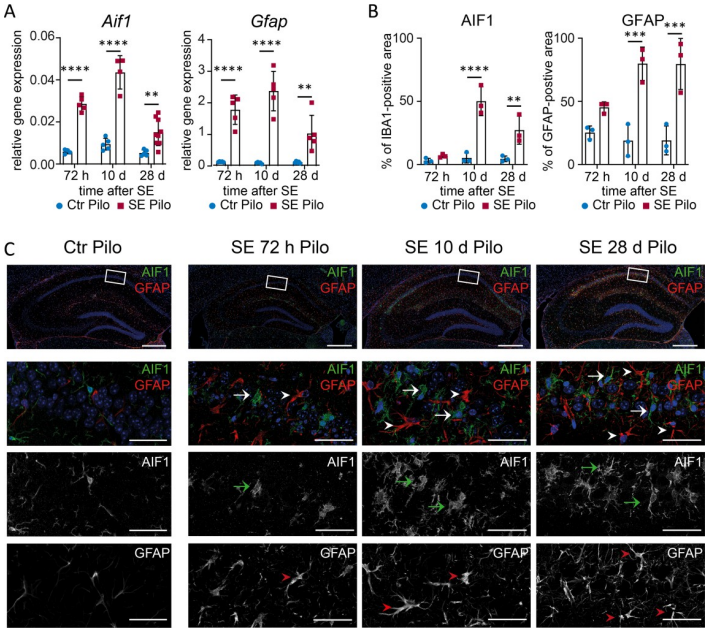

Fig 4. Sustained microglial activation and astrogliosis after pilocarpine-induced SE. (**A**) mRNA level of Aif1 (microglia) and Gfap (astrocytes) are analysed 72 h ($n \geq 5$), 10 d ($n \geq 4$) and 28 d ($n \geq 6$) after pilocarpine-induced SE (SE Pilo) compared to non-SE control animals (Ctr Pilo) using the housekeeping gene β-actin ($\Delta\Delta C_t$ method). (**B**) Semi-quantitative analysis of AIF1- or GFAP-positive area reveal a progressive increase over time in CA1 (all groups n = 3). Data is analysed with 2way ANOVA followed by Sidak's post hoc test. Asterisks indicate significant differences between groups (control vs. SE): $^{*}p < 0.05$, $^{**}p < 0.01$, $^{***}p < 0.001$, $^{****}p < 0.0001$. Detailed statistical values are supported in S2 Table. (**C**) Single AIF1 positive cells (green) can be found 72 h after SE with an increasing number 10 d and 28 d post-SE (arrows). GFAP positive astrocytes (red) with enlarged stem processes are increasingly distributed over the hippocampal section with disease progression (arrowheads). In non-SE control animals (leftmost panels, Ctr Pilo), only single ramified microglia and non-overlapping astrocytes with very fine processes can be found. Scale bars: 500 μm (overview), 50 μm (insert). DAPI for nucleic acid counterstain (blue).

https://doi.org/10.1371/journal.pone.0271995.g004

enlarged stem processes were observed 72 hours and 10 days post-SE indicating a mild to moderate astrogliosis (Fig 4C), classified according to Sofroniew [39] (S2 Fig). In the chronic state (28 days after SE), abundant astrocytes were detectable, leading to an overlap of astrocytic cellular processes. However, the cell bodies and processes were less prominent, which points towards a less reactive state. In non-SE control animals, single ramified microglia and non-overlapping astrocytes with very fine processes were detected (Fig 4C).

In contrast to the pilocarpine model, only a transiently augmented expression of *Aif1* was present 72 hours and 10 days after disease onset (Fig 5A, leftmost) in the KA-model. *Gfap* mRNA was increased at 72 hours and 28 days, but not 10 days after SE (Fig 5A, rightmost). In addition, semi-quantitative analysis of astrocytic and microglial activation revealed an increasing volume of these cell types during the model progression in the ipsilateral CA1 region (Fig 5B), whereas the contralateral CA1 was mostly unaffected (S1B Fig). An increase in microglia was only evident contralaterally in the later model phase (28 days), possibly as a late secondary immune response. Different stages of microglia activation (ramified, hypertrophic, bushy, and amoeboid) were observed after KA-induced SE (S2 Fig). In contrast, rod and single ramified non-activated microglia could be found in non-SE controls (Fig 5C). A diffuse accumulation of activated bushy microglia was seen already 72 hours after SE in the entire ipsilateral hippocampal formation (Fig 5C), whereas 10 days after SE, amoeboid and bushy shaped microglia appeared in a more clustered and condensed pattern in the CA1 region. In the contralateral hippocampal formation, the microglia appeared in amoeboid shapes (Fig 5D). Interestingly, 10 days after SE microglia returned to a non-activated ramified morphology, as observed in non-SE controls. At 28 days post SE, a dense network of amoeboid shaped microglia was observed, clustered in CA1 and subiculum. Astrocytes (Fig 5C) appeared non-overlapping with hypertrophy of stem processes within the entire hippocampal area 72 hours after SE, indicating a mild to moderate astrogliosis. Ten days after SE, the number of astrocytes increased mainly in CA1 and DG of the ipsilateral hippocampus. Reactive astrocytes showed overlapping cell processes and some cell bodies exhibited corresponding signs of hypertrophy, whereas others lost individual domains, representing a severe diffuse astrogliosis [39]. Contralateral to the injection side, only a few astrocytes with slightly thickened stem processes could be observed (Fig 5D). Four weeks after SE, astrogliosis on the ipsilateral side spread from the respective areas (CA1 and DG) and included the entire hippocampal formation. Astrocytes in the ipsilateral CA1 region presented elongated shapes and overlapping processes, demonstrating a severe astrogliosis with compact scar formation. In the contralateral hippocampal formation, numerous hypertrophic astrocytes indicative of a severe diffuse astrogliosis were found in the CA1 region (Fig 5D).

Robust expression of NLRP3 associated transcripts is independent of neuronal damage

Hippocampal biopsy specimen of TLE patients (Fig 6A, H. & E.) who underwent surgical removal of the affected hippocampal formation for seizure relief, demonstrated distinct neuropathological features. HS-TLE is presented with a considerably stronger structural reorganization and neuronal cell loss compared to lesion-associated TLE (Fig 6A, NeuN). Further immunohistochemical analysis showed an extensive astrogliosis in HS-TLE hippocampi, but only mild to moderate stages in lesion-associated TLE hippocampi (Fig 6B, GFAP). Microglia infiltration was observed by AIF1 immunohistochemistry in all TLE hippocampi, independently of the neuropathological phenotype (Fig 6B, AIF1). Additional immunolabeling against NLRP3 also revealed a similar expression pattern in both TLE pathologies evaluated by morphological analysis (Fig 6C).

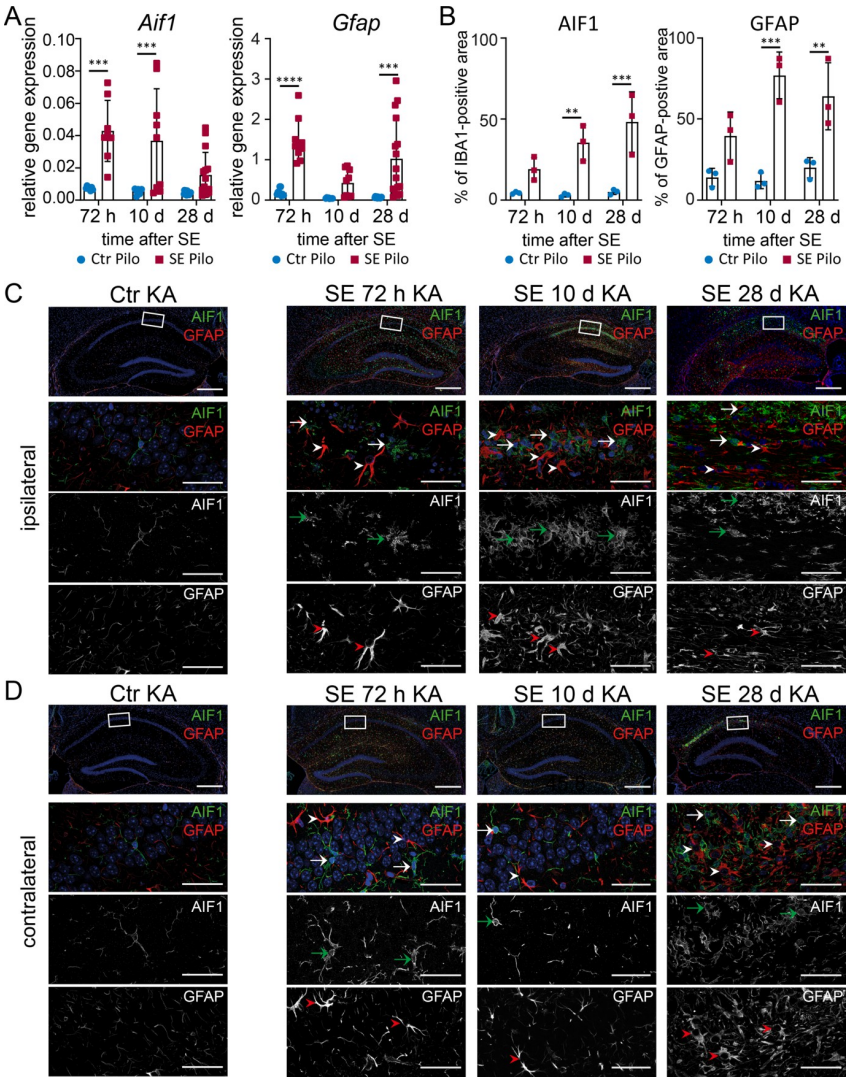

Fig 5. Astrogliosis and microglial activation are persistent after kainic acid-induced SE. (A) mRNA level of Aif1 and Gfap are determined 72 h ($n \geq 4$), 10 d ($n \geq 5$) and 28 d ($n \geq 6$) after SE using the housekeeping gene β-actin ($\Delta\Delta C_t$ method). (B) Semi-quantitative analysis of AIF1- or GFAP-positive area reveal a progressive increase over time in the ipsilateral CA1 (all groups n = 3). Data is analysed with 2way ANOVA followed by Sidak's post hoc test. Asterisks indicate significant differences between groups: $^{*}p < 0.05$, $^{**}p < 0.01$, $^{***}p < 0.001$, $^{****}p < 0.0001$. Detailed statistical values are supported in S2 Table. (C) AIF1 (green) positive microglial cells are manifested in the hippocampus post-SE primarily presented with a bushy morphology (arrows) becoming bushier. GFAP positive cells (red) with prominent stem processes are equally scattered over the hippocampal area (arrowheads) mainly found in the CA1 and DG region, with cell processes overlapping to a high degree. In non-SE control animals, a few ramified microglia are observed (leftmost). GFAP positive cells are similarly scarce and presented with very narrow cell processes. Scale bars: 500 μm (overview), 50 μm (insert). DAPI for nucleic acid counterstain in blue.

https://doi.org/10.1371/journal.pone.0271995.g005

When proinflammatory reorganization was analysed on the cellular level by RNA sequencing (Fig 6D), HS-TLE tissue revealed a significantly increased GFAP expression compared to lesion-associated TLE indicating a higher number of reactive astrocytes. In contrast, accordingly to the protein expression, *Aif1* mRNA, a marker for microglia, was not differentially expressed between the two groups. Additionally, we analysed gene expression of NLRP3 pathway components. The majority of genes (namely *Nlrp3*, *Casp1*, *NfkB2*, *Il1b* and *Il18*) did not

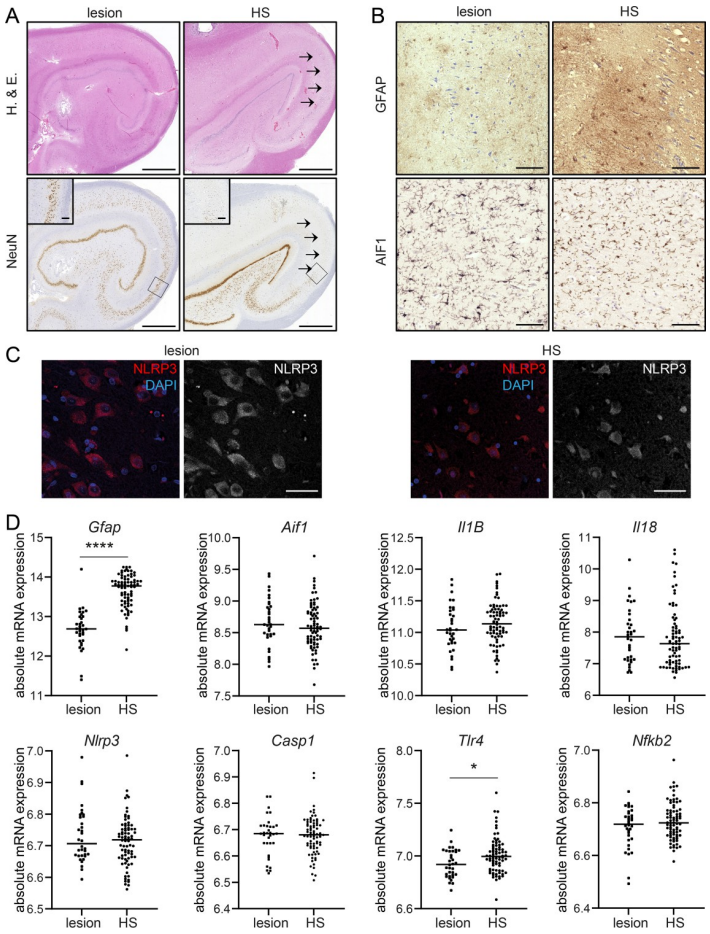

Fig 6. Activation of NLRP3-signalling associated genes in human TLE hippocampi. (**A**) Representative NeuN immunohistochemistry reveals a classical pattern for HS-TLE with segmental neuronal loss pronounced in CA1 (rightmost, arrows) whereas neurons are well conserved in the lesion-associated hippocampus. Scale bars: 500 μm (overview), 100 μm (insert). (**B**) Only scattered astrocytes are observed in lesion-associated TLE (leftmost, see inserts), compared with pronounced fibrillary reactive astrogliosis in HS-TLE (leftmost). Similar reactivity of activated microglia (AIF1) is observed in both pathologies (lower panels). Scale bars: 100 μm. (**C**) Representative NLRP3 immunolabeling also shows a similar expression pattern in both TLE forms. Scale bars: 50 μm. (**D**) mRNA level of *Gfap*, *Aif1*, *Il1B*, *Il18*, *Nlrp3*, *Casp1*, *Tlr4 and Nfkb2* are determined with RNA sequencing in HS-TLE (n = 78) and lesion-associated TLE patients (n = 34). Data is analysed with Mann-Whitney U test. Asterisks indicate significant differences between groups: $^{*}p < 0.05$, $^{****}p < 0.0001$.

https://doi.org/10.1371/journal.pone.0271995.g006

show a difference between HS and lesion-associated pathology. However, *Tlr4* mRNA was significantly augmented in HS-TLE hippocampi (Fig 6D).

Discussion

Here, we have comparatively analysed the dynamics of inflammasomal pathway components after distinct transient insults. Our data suggest fundamental differences dependent of the particular stimulus, i.e., systemic pilocarpine versus suprahippocampal KA. It has to be noted that molecular activation patterns can be affected by specific pharmacological induction triggering the immediate pharmacological effects on immunological signalling. Pilocarpine acts directly on Caspase-1/IL-1β signalling, in particular at muscarinic M3 receptors and thus impacts on microglia as they express functional muscarinic receptors [40, 41]. KA has been demonstrated

to activate inflammasomal molecules via binding to Girk1 and other KA-receptors and to induce endoplasmatic reticulum stress [42]. However, the effects of two key factors–SE *and* immediate pharmacological signalling—are virtually indistinguishable in the present models. Thus, the differences between the pilocarpine- and KA-induced SE models in terms of different activation profiles of inflammasome-related molecules suggest distinct and specific dynamics of inflammasome signalling dependent on the stimulus.

Previous animal studies have shown an augmentation and activation of NLRP3 pathway proteins as an acute response to chemoconvulsant and electrically kindling-induced SE (24–72 h post SE) [12, 13, 25, 43]. We investigated the gene expression pattern over a four week period in two chemoconvulsant models, which are known to replicate the neuropathological features found most commonly in human TLE: hippocampal sclerosis with extensive neuronal death and structural reorganization [6]. In the pilocarpine model, mice show a prolonged inflammatory response, which is still present at 10 d after SE, but not in the later chronic phase (28 days). However, mice in the KA-model present with a biphasically appearing inflammatory activation, showing an augmentation of proinflammatory mRNA at 72 h post SE as well as in the later chronic model stage although seizure frequency remains stable until week 6 after SE in this model [27]. Previous animal studies have shown an augmentation and activation of NLRP3 pathway proteins as an acute response to chemoconvulsant and electrically kindling-induced SE (24–72 h post SE) [12, 13, 25, 43]. For IL1B expression, in line with previous findings after pilocarpine-induced SE in rats [44], we observed immunoreactivity at all investigated time points. We observed a shift from mainly neuronal IL1B expression at early stages (72 h post SE) to glial expression at later stages (10 d and 28 d post SE) in both models. Early neuronal IL1B expression may be a response to excitotoxic cell damage. Whereas neuronal IL1B expression in the KA model showed a broad dispersion across CA1, it appeared to be spatially clustered only in a small number of neurons in the pilocarpine model. Clustered expression of IL1B in neurons associated with TLE has been shown previously in rats after electrically induced SE within the stimulated CA3 region [45]. We hypothesize that SE induced by systemic administration of pilocarpine leads to indirect neuronal damage by hyperexcitation, and thus to a clustered pattern of damage. In contrast, local application of kainic acid above the CA1 region leads to a more widespread direct toxic effect on neurons [46] resulting in broad neuronal activation throughout the CA1 region. This may then induce a diffuse inflammation and IL1B expression in the CA1 area that is severe enough to be detectable by mRNA quantification. In contrast, in the pilocarpine model, neurons have been shown to form spatially restricted functional clusters [47] with segmental neuronal cell loss as a common hallmark [48, 49], which can be detected already 2 days after pilocarpine-induced SE in the CA1 region [48, 50].

Hippocampi after pilocarpine-induced SE as well as the ipsilateral hippocampus after suprahippocampal KA-induced SE show extensive neuronal damage. Thus, we speculated whether neurodegeneration, e.g., via release of cell death-associated molecules, may be critical in stimulating inflammasomal signalling. However, the lack of significant differences in the expression of inflammasome-associated signals between the ipsi- and contralateral (less damaged) hippocampal formation in KA-exposed mice suggest that seizure activity itself appears to be the most important factor in active inflammasomal signalling.

With respect to the role in human TLE, NLRP3 and associated proteins (CASP1, ASC, IL1B) have been shown to be upregulated in hippocampi of patients with pharmacoresistant TLE [12, 24, 25]. However, these studies have focussed on analysing inflammasome signalling in human hippocampi with the damage pattern of HS. Comparisons between expression patterns in biopsies from epilepsy surgery in pharmacoresistant patients with HS *plus* epileptogenesis with lesion-associated TLE and absent segmental neurodegeneration *without* epileptogenesis [4, 6] may provide important information about the role of pathomechanisms

for distinct aspects of human TLE [30]. Due to the general absence of matching non-epileptic human control tissue, the comparison of neuropathological and molecular properties between HS and lesion-associated human TLE is used to gain a better understanding of underlying pathogenetic mechanisms [6, 30].

Our present data clearly demonstrate that in chronic human TLE hippocampi there is robust and largely indistinguishable expression of key inflammasome components independent of both, the neurodegenerative state and the extent and type of astrogliosis. Only expression of Tlr4 was significantly increased in HS versus lesion-associated hippocampi. This finding is well in line with previous data demonstrating the importance of the HMGB1-TLR4 axis for this type of TLE pathology [11]. Our data indicate a certain level of specificity for this mechanism in HS- compared to lesion-associated TLE, which is also supported by the previously described positive correlation of Tlr4 expression levels in HS hippocampi with seizure activity [34].

Activated microglia and reactive astrocytes are associated with release of proinflammatory cytokines in human and experimental TLE [23, 36, 37, 51]. Furthermore, these cell types have been shown to contribute to epileptogenesis in experimental models [9, 52]. We analysed *Aif1* and *Gfap* mRNA as well as protein localization to determine the timeline of more general proinflammatory changes in both animal models and human chronic TLE. As to be expected, HS-TLE patients present with a stronger structural reorganization, neuronal cell loss and astrogliosis compared to lesion-associated TLE patients. However, microglia infiltration or NLRP3 expression does not differ between the two pathologies. Concordant to the time line of the more specific (NLRP3 pathway-related) findings in our experimental models, highest mRNA expression and more 'activated' cell morphology for both microglia and astrocytes is found at 10 days post SE in the pilocarpine model. In the later chronic phase, densely packed and highly activated microglia and astrocytes along with increased *Gfap* and *Aif1* mRNA levels are found in the KA-model. A study focussing on even later time points in the suprahippocampal KA-model shows that astrocyte-related pathogenic changes are progressing up to nine month post-SE [9]. The time lag between mRNA generation and protein expression at day 10 in the KA model might be due to the highly variable and complex translational processes [53]. Post-translational modifications, such as phosphorylation, which important for protein stability and function, also happen on different time scales [54]. Consequently, the expression of both, mRNA and protein, may vary at the same time point.

Thus, an important finding arising from this study is a potentially distinct mechanism causing diverse time courses of inflammatory activity in the two different mouse models with similar seizure frequency during various model stages [9, 28, 29, 55]. The biphasic inflammatory timeline in the KA model could be attributed initially to an acute response to excitotoxicity and SE, with an ongoing chronic progression of inflammation and cellular remodelling, eventually leading to destruction of the hippocampal formation. Potentially, these chronic pathogenetic changes could be caused by self-perpetuating inflammatory cascades (such as the NLRP3 pathway). Another possibility is an association of IL1B driven chronic neuroinflammation with increased seizure frequency. Different studies report a progression of seizure frequency in the KA-model [9, 56, 57] which we could confirm. In contrast, a lasting increase in seizure frequency in the pilocarpine model is detected just for subgroups of animals [7, 58] with low but stable seizure occurrence in the later phase [28, 29]. It has been shown that IL1B contributes to hyperexcitability [59], which gives rise to the hypothesis that inflammatory processes in the chronic state after KA- induced SE could promote an increase in seizure frequency. Although a direct correlation between seizure frequency and gene expression was only found for Il1b in the KA model, this does not argue against a dependence of both parameters. Seizure frequency is extremely variable inter-individually, so a comprehensive transcriptional analysis with

individual seizure frequency should be considered for a solid analysis. Moreover, it is also possible that the changes in the expression of the NLRP3-associated genes are secondary phenomena of the epileptogenic process, for instance, due to altered cell composition or cytokine accumulation in brain tissue, rather than a direct consequence of altered neuronal balance.

In summary, our data from human and experimental TLE hippocampi suggest that inflammasome pathway activation and seizure activity are inextricably linked in the manifestation of a chronic epileptic state. Given the highly dynamic epileptogenic transcript profiles that depend on the particular insult modalities, further research is needed to address highly specific, distinct molecular components of inflammasome signalling in a therapeutic context for pharmacoresistant TLE.

Supporting information

S1 Fig. No difference in mRNA expression of inflammasomal related genes is observed between ipsi- and contralateral CA1 region after KA-induced SE. (**A**) Relative mRNA levels ($\Delta\Delta C_t$ method) are analysed 72 h ($n \geq 4$), 5 d ($n \geq 5$), 10 d ($n \geq 4$) and 28 d ($n \geq 6$) after kainic acid-induced SE comparing ipsi- and contralateral CA1 with 2way ANOVA followed by Sidak's post hoc test. The ubiquitously expressed *β-actin* is used as housekeeping gene. (**B**) Semi-quantitative analysis of AIF1- or GFAP-positive area reveal nearly no significant changes over time in the contralateral CA1 (all groups n = 3) with 2way ANOVA followed by Sidak's post hoc test. An increase in microglia (AIF1) was only evident contralaterally in the later model phase (28 days). Asterisks indicate significant differences between groups: $^{*}p < 0.05$. Detailed statistical values are found in S2 Table.
(TIF)

S2 Fig. Different cell shapes of microglia and astrocytes. (**A**) Visualisation of AIF1 positive microglia (green) and (**B**) GFAP positive astrocytes (red) presenting different shapes of soma and projections depending on the activation status after SE. Scale bars: 20 μm.
(TIF)

S3 Fig. Almost no correlation between seizure frequency and gene expression. (A, B) Median of the summarized seizure frequency of three consecutive days before mRNA analysis for every animal after (**A**) pilocarpine (n = 11) and (**B**) KA-induced SE (n = 21) correlated to mRNA expression level of representative genes. (**C, D**) Simple regression analysis of seizure frequency and mRNA gene expression of three representative genes analysed after (**C**) pilocarpine and (**D**) KA-induced SE. Asterisks indicate significant differences between groups: $^{*}p < 0.05$. Detailed statistical values are found in S2 Table.
(TIF)

S1 Table. Distribution of clinical parameters with the "lesion associated" and hippocampal sclerosis (HS) patient groups. LEV = Levetiracetam. Engel class IA: completely seizure free; class IVB: no seizure freedom.
(PDF)

S2 Table. Statistical analysis.
(PDF)

Acknowledgments

We thank Pia Trebing and Sabine Opitz for excellent technical assistance. The Department of Epileptology is a full member of the ERN EpiCARE.

Author Contributions

Conceptualization: Thoralf Opitz, Rainer Surges, Motaz Hamed, Hartmut Vatter, Susanne Schoch, Albert J. Becker, Julika Pitsch.

Data curation: Malin S. Pohlentz, Silvia Cases-Cunillera.

Formal analysis: Malin S. Pohlentz, Silvia Cases-Cunillera, Thoralf Opitz, Susanne Schoch, Julika Pitsch.

Funding acquisition: Susanne Schoch, Albert J. Becker, Julika Pitsch.

Investigation: Philipp Müller, Albert J. Becker, Julika Pitsch.

Methodology: Philipp Müller, Motaz Hamed, Hartmut Vatter, Susanne Schoch.

Project administration: Albert J. Becker, Julika Pitsch.

Resources: Motaz Hamed, Hartmut Vatter.

Supervision: Albert J. Becker, Julika Pitsch.

Validation: Philipp Müller, Rainer Surges, Susanne Schoch, Julika Pitsch.

Visualization: Malin S. Pohlentz, Silvia Cases-Cunillera, Julika Pitsch.

Writing – original draft: Malin S. Pohlentz, Silvia Cases-Cunillera, Thoralf Opitz, Susanne Schoch, Albert J. Becker, Julika Pitsch.

Writing – review & editing: Malin S. Pohlentz, Thoralf Opitz, Rainer Surges, Motaz Hamed, Hartmut Vatter, Susanne Schoch, Albert J. Becker, Julika Pitsch.

References

1. Asadi-Pooya AA, Stewart GR, Abrams DJ, Sharan A. Prevalence and Incidence of Drug-Resistant Mesial Temporal Lobe Epilepsy in the United States. Vol. 99, World Neurosurgery. 2017. p. 662–6. https://doi.org/10.1016/j.wneu.2016.12.074 PMID: 28034810
2. Pitkänen A, Engel J. Past and Present Definitions of Epileptogenesis and Its Biomarkers. Neurotherapeutics. 2014. p. 231–241. https://doi.org/10.1007/s13311-014-0257-2 PMID: 24492975
3. Vakharia VN, Duncan JS, Witt JA, Elger CE, Staba R, Engel J. Getting the best outcomes from epilepsy surgery. Vol. 83, Annals of Neurology. John Wiley and Sons Inc.; 2018. p. 676–90. https://doi.org/10.1002/ana.25205 PMID: 29534299
4. Blümcke I, Thom M, Aronica E, Armstrong DD, Bartolomei F, Bernasconi A, et al. International consensus classification of hippocampal sclerosis in temporal lobe epilepsy: A Task Force report from the ILAE Commission on Diagnostic Methods. Epilepsia. 2013; 54(7):1315–29. https://doi.org/10.1111/epi.12220 PMID: 23692496
5. Johnson AM, Sugo E, Barreto D, Hiew CC, Lawson JA, Connolly AM, et al. The Severity of Gliosis in Hippocampal Sclerosis Correlates with Pre-Operative Seizure Burden and Outcome After Temporal Lobectomy. Mol Neurobiol. 2016; 53(8):5446–56. https://doi.org/10.1007/s12035-015-9465-y PMID: 26452360
6. Becker AJ. Review: Animal models of acquired epilepsy: insights into mechanisms of human epileptogenesis. Neuropathol Appl Neurobiol. 2018 Feb; 44(1):112–29. https://doi.org/10.1111/nan.12451 PMID: 29130506
7. Cavalheiro EA, Santos NF, Priel MR. The pilocarpine model of epilepsy in mice. Epilepsia. 1996 Oct; 37(10):1015–9. https://doi.org/10.1111/j.1528-1157.1996.tb00541.x PMID: 8822702
8. Duran RV, Bastos EM, Arashiro DK, Gorgulho A, Purcelli M, Rivero RL, et al. Status epilepticus and spontaneous seizures in the pilocarpine and kainic acid models of epilepsy. Soc Neurosci. 1993; 19:394.
9. Bedner P, Dupper A, Hüttmann K, Müller J, Herde MK, Dublin P, et al. Astrocyte uncoupling as a cause of human temporal lobe epilepsy. Brain. 2015 May 1; 138(5):1208–22. https://doi.org/10.1093/brain/awv067 PMID: 25765328

10. Vezzani A, Rüegg S. The pivotal role of immunity and inflammatory processes in epilepsy is increasingly recognized: introduction. Epilepsia. 2011 May; 52 Suppl 3:1–4. https://doi.org/10.1111/j.1528-1167.2011.03028.x PMID: 21542838

11. Maroso M, Balosso S, Ravizza T, Liu J, Aronica E, Iyer A, et al. Toll-like receptor 4 and high-mobility group box-1 are involved in ictogenesis and can be targeted to reduce seizures. Nat Med. 2010 Apr; 16 (4):413–9. https://doi.org/10.1038/nm.2127 PMID: 20348922

12. Wu C, Zhang G, Chen L, Kim S, Yu J, Hu G, et al. The Role of NLRP3 and IL-1β in Refractory Epilepsy Brain Injury. Front Neurol. 2020; 10(February):1–8. https://doi.org/10.3389/fneur.2019.01418 PMID: 32116990

13. Meng XF, Tan L, Tan MS, Jiang T, Tan CC, Li MM, et al. Inhibition of the NLRP3 inflammasome provides neuroprotection in rats following amygdala kindling-induced status epilepticus. J Neuroinflammation. 2014; 11(1):212. https://doi.org/10.1186/s12974-014-0212-5 PMID: 25516224

14. Vezzani A, Viviani B. Neuromodulatory properties of inflammatory cytokines and their impact on neuronal excitability. Neuropharmacology. 96(Pt A):70–82. https://doi.org/10.1016/j.neuropharm.2014.10.027 PMID: 25445483

15. Maroso M, Balosso S, Ravizza T, Iori V, Wright CI, French J, et al. Interleukin-1β Biosynthesis Inhibition Reduces Acute Seizures and Drug Resistant Chronic Epileptic Activity in Mice. Neurotherapeutics. 2011; 8(2):304–15. https://doi.org/10.1007/s13311-011-0039-z PMID: 21431948

16. Bauernfeind FG, Horvath G, Stutz A, Alnemri ES, MacDonald K, Speert D, et al. Cutting Edge: NF-κB Activating Pattern Recognition and Cytokine Receptors License NLRP3 Inflammasome Activation by Regulating NLRP3 Expression. J Immunol. 2009; 183(2):787–91.

17. Schroder K, Tschopp J. The Inflammasomes. Cell. 2010; 140(6):821–32. https://doi.org/10.1016/j.cell.2010.01.040 PMID: 20303873

18. Bergsbaken T, Fink SL, den Hartigh AB, Loomis WP, Cookson BT. Coordinated Host Responses during Pyroptosis: Caspase-1–Dependent Lysosome Exocytosis and Inflammatory Cytokine Maturation. J Immunol. 2011; 187(5):2748–54. https://doi.org/10.4049/jimmunol.1100477 PMID: 21804020

19. Vezzani A, Balosso S, Ravizza T. The role of cytokines in the pathophysiology of epilepsy. Brain Behav Immun. 2008 Aug; 22(6):797–803. https://doi.org/10.1016/j.bbi.2008.03.009 PMID: 18495419

20. Vezzani A, Moneta D, Conti M, Richichi C, Ravizza T, De Luigi A, et al. Powerful anticonvulsant action of IL-1 receptor antagonist on intracerebral injection and astrocytic overexpression in mice. Proc Natl Acad Sci U S A. 2000; 97(21):11534–9. https://doi.org/10.1073/pnas.190206797 PMID: 11016948

21. Iori V, Iyer AM, Ravizza T, Beltrame L, Paracchini L, Marchini S, et al. Blockade of the IL-1R1/TLR4 pathway mediates disease-modification therapeutic effects in a model of acquired epilepsy. Neurobiol Dis. 2017 Mar; 99:12–23. https://doi.org/10.1016/j.nbd.2016.12.007 PMID: 27939857

22. Crespel A, Coubes P, Rousset MC, Brana C, Rougier A, Rondouin G, et al. Inflammatory reactions in human medial temporal lobe epilepsy with hippocampal sclerosis. Brain Res. 2002 Oct 18; 952(2):159–69. https://doi.org/10.1016/s0006-8993(02)03050-0 PMID: 12376176

23. Leal B, Chaves J, Carvalho C, Rangel R, Santos A, Bettencourt A, et al. Brain expression of inflammatory mediators in Mesial Temporal Lobe Epilepsy patients. J Neuroimmunol. 2017 Dec 15; 313:82–8. https://doi.org/10.1016/j.jneuroim.2017.10.014 PMID: 29153613

24. Cristina de Brito Toscano E, Leandro Marciano Vieira É, Boni Rocha Dias B, Vidigal Caliari M, Paula Gonçalves A, Varela Giannetti A, et al. NLRP3 and NLRP1 inflammasomes are up-regulated in patients with mesial temporal lobe epilepsy and may contribute to overexpression of caspase-1 and IL-β in sclerotic hippocampi. Brain Res. 2021; 1752(Feb):147230. https://doi.org/10.1016/j.brainres.2020.147230 PMID: 33385378

25. Yue J, Wei YJ, Yang XL, Liu SY, Yang H, Zhang CQ. NLRP3 inflammasome and endoplasmic reticulum stress in the epileptogenic zone in temporal lobe epilepsy: molecular insights into their interdependence. Neuropathol Appl Neurobiol. 2020; 46(7):779–85. https://doi.org/10.1111/nan.12621 PMID: 32311777

26. Sharma AK, Reams RY, Jordan WH, Miller MA, Thacker HL, Snyder PW. Mesial temporal lobe epilepsy: Pathogenesis, induced rodent models and lesions. Toxicol Pathol. 2007; 35(7):984–99. https://doi.org/10.1080/01926230701748305 PMID: 18098044

27. Pitsch J, Kuehn JC, Gnatkovsky V, Müller JA, van Loo KMJ, de Curtis M, et al. Anti-epileptogenic and Anti-convulsive Effects of Fingolimod in Experimental Temporal Lobe Epilepsy. Mol Neurobiol. 2019 Mar 22; 56(3):1825–40. https://doi.org/10.1007/s12035-018-1181-y PMID: 29934763

28. Pitsch J, Opitz T, Borm V, Woitecki A, Staniek M, Beck H, et al. The presynaptic active zone protein rim α controls epileptogenesis following status epilepticus. J Neurosci. 2012; 32(36):12384–95.

29. Pitsch J, Becker AJ, Schoch S, Müller JA, de Curtis M, Gnatkovsky V. Circadian clustering of spontaneous epileptic seizures emerges after pilocarpine-induced status epilepticus. Epilepsia. 2017; 58 (7):1159–71. https://doi.org/10.1111/epi.13795 PMID: 28542864

30. Van Loo KMJ, Schaub C, Pitsch J, Kulbida R, Opitz T, Ekstein D, et al. Zinc regulates a key transcriptional pathway for epileptogenesis via metal-regulatory transcription factor 1. Nat Commun. 2015; 6:8688. https://doi.org/10.1038/ncomms9688 PMID: 26498180

31. Kral T, Clusmann H, Urbach J, Schramm J, Elger C, Kurthen M, et al. Preoperative evaluation for epilepsy surgery (Bonn Algorithm). Zentralbl Neurochir. 2002; 63(3):106–10. https://doi.org/10.1055/s-2002-35826 PMID: 12457335

32. Blümcke I, Pauli E, Clusmann H, Schramm J, Becker A, Elger C, et al. A new clinico-pathological classification system for mesial temporal sclerosis. Acta Neuropathol. 2007 Mar; 113(3):235–44. https://doi.org/10.1007/s00401-006-0187-0 PMID: 17221203

33. Becker AJ, Chen J, Zien A, Sochivko D, Normann S, Schramm J, et al. Correlated stage- and subfield-associated hippocampal gene expression patterns in experimental and human temporal lobe epilepsy. Eur J Neurosci. 2003 Nov; 18(10):2792–802. https://doi.org/10.1111/j.1460-9568.2003.02993.x PMID: 14656328

34. Pernhorst K, Herms S, Hoffmann P, Cichon S, Schulz H, Sander T, et al. TLR4, ATF-3 and IL8 inflammation mediator expression correlates with seizure frequency in human epileptic brain tissue. Seizure. 2013 Oct; 22(8):675–8. https://doi.org/10.1016/j.seizure.2013.04.023 PMID: 23706953

35. Pitsch J, Schoch S, Gueler N, Flor PJ, van der Putten H, Becker AJ. Functional role of mGluR1 and mGluR4 in pilocarpine-induced temporal lobe epilepsy. Neurobiol Dis. 2007 Jun; 26(3):623–33. https://doi.org/10.1016/j.nbd.2007.03.003 PMID: 17446080

36. Bauer J, Becker AJ, Elyaman W, Peltola J, Rüegg S, Titulaer MJ, et al. Innate and adaptive immunity in human epilepsies. Epilepsia. 2017 Jul 1; 58:57–68. https://doi.org/10.1111/epi.13784 PMID: 28675562

37. Rizzi M, Perego C, Aliprandi M, Richichi C, Ravizza T, Colella D, et al. Glia activation and cytokine increase in rat hippocampus by kainic acid-induced status epilepticus during postnatal development. Neurobiol Dis. 2003; 14(3):494–503. https://doi.org/10.1016/j.nbd.2003.08.001 PMID: 14678765

38. Wyatt-Johnson SK, Herr SA, Brewster AL. Status Epilepticus Triggers Time-Dependent Alterations in Microglia Abundance and Morphological Phenotypes in the Hippocampus. Front Neurol. 2017 Dec 18; 8(DEC). https://doi.org/10.3389/fneur.2017.00700 PMID: 29326654

39. Sofroniew M V. Astrogliosis. Cold Spring Harb Perspect Biol. 2014; 7(2):a020420. https://doi.org/10.1101/cshperspect.a020420 PMID: 25380660

40. Pannell M, Meier MA, Szulzewsky F, Matyash V, Endres M, Kronenberg G, et al. The subpopulation of microglia expressing functional muscarinic acetylcholine receptors expands in stroke and Alzheimer's disease. Brain Struct Funct. 2016 Mar 1; 221(2):1157–72. https://doi.org/10.1007/s00429-014-0962-y PMID: 25523105

41. Wang S, Jiang Y, Chen J, Dai C, Liu D, Pan W, et al. Activation of M 3 muscarinic acetylcholine receptors delayed cardiac aging by inhibiting the Caspase-1/IL-1β Signaling Pathway. Cell Physiol Biochem. 2018 Oct 1; 49(3):1249–57.

42. Zheng XY, Lv YD, Jin FY, Wu XJ, Zhu J, Ruan Y. Kainic acid hyperphosphorylates tau via inflammasome activation in MAPT transgenic mice. Aging (Albany NY). 2019; 11(23):10923–38. https://doi.org/10.18632/aging.102495 PMID: 31789603

43. Jiang J, Yang M soon, Quan Y, Gueorguieva P, Ganesh T, Dingledine R. Therapeutic window for cyclooxygenase-2 related anti-inflammatory therapy after status epilepticus. Neurobiol Dis. 2015 Apr 1; 76:126–36. https://doi.org/10.1016/j.nbd.2014.12.032 PMID: 25600211

44. Ravizza T, Gagliardi B, Noé F, Boer K, Aronica E, Vezzani A. Innate and adaptive immunity during epileptogenesis and spontaneous seizures: evidence from experimental models and human temporal lobe epilepsy. Neurobiol Dis. 2008 Jan; 29(1):142–60. https://doi.org/10.1016/j.nbd.2007.08.012 PMID: 17931873

45. De Simoni MG, Perego C, Ravizza T, Moneta D, Conti M, Marchesi F, et al. Inflammatory cytokines and related genes are induced in the rat hippocampus by limbic status epilepticus. Eur J Neurosci. 2000; 12(7):2623–33. https://doi.org/10.1046/j.1460-9568.2000.00140.x PMID: 10947836

46. Vezzani A, Conti M, De Luigi A, Ravizza T, Moneta D, Marchesi F, et al. Interleukin-1beta immunoreactivity and microglia are enhanced in the rat hippocampus by focal kainate application: functional evidence for enhancement of electrographic seizures. J Neurosci. 1999 Jun 15; 19(12):5054–65. https://doi.org/10.1523/JNEUROSCI.19-12-05054.1999 PMID: 10366638

47. Muldoon SF, Soltesz I, Cossart R. Spatially clustered neuronal assemblies comprise the microstructure of synchrony in chronically epileptic networks. Proc Natl Acad Sci [Internet]. 2013 Feb 26 [cited 2021 Nov 3]; 110(9):3567–72. Available from: https://www.pnas.org/content/110/9/3567 https://doi.org/10.1073/pnas.1216958110 PMID: 23401510

48. Becker AJ, Pitsch J, Sochivko D, Opitz T, Staniek M, Chen CC, et al. Transcriptional upregulation of Cav3.2 mediates epileptogenesis in the pilocarpine model of epilepsy. J Neurosci. 2008. https://doi.org/10.1523/JNEUROSCI.1421-08.2008 PMID: 19052226

49. Mello LEAM, Cavalheiro EA, Tan AM, Kupfer WR, Pretorius JK, Babb TL, et al. Circuit mechanisms of seizures in the pilocarpine model of chronic epilepsy: cell loss and mossy fiber sprouting. Epilepsia. 1993; 34(6):985–95. https://doi.org/10.1111/j.1528-1157.1993.tb02123.x PMID: 7694849

50. Covolan L, Mello LEAM. Temporal profile of neuronal injury following pilocarpine or kainic acid-induced status epilepticus. Epilepsy Res. 2000; 39(2):133–52. https://doi.org/10.1016/s0920-1211(99)00119-9 PMID: 10759302

51. Vezzani A, Moneta D, Richichi C, Aliprandi M, Burrows SJ, Ravizza T, et al. Functional role of inflammatory cytokines and antiinflammatory molecules in seizures and epileptogenesis. Epilepsia. 2002; 43 (SUPPL. 5):30–5. https://doi.org/10.1046/j.1528-1157.43.s.5.14.x PMID: 12121291

52. Zhao X, Liao Y, Morgan S, Gruenthal M, Zhao X, Liao Y, et al. Noninflammatory Changes of Microglia Are Sufficient to Cause Epilepsy. CellReports. 2018; 22(8):2080–93. https://doi.org/10.1016/j.celrep.2018.02.004 PMID: 29466735

53. Ingolia NT, Lareau LF, Weissman JS. Ribosome profiling of mouse embryonic stem cells reveals the complexity and dynamics of mammalian proteomes. Cell. 2011 Nov 11; 147(4):789–802. https://doi.org/10.1016/j.cell.2011.10.002 PMID: 22056041

54. Ramazi S, Zahiri J. Posttranslational modifications in proteins: resources, tools and prediction methods. Database (Oxford). 2021; 2021. https://doi.org/10.1093/database/baab012 PMID: 33826699

55. Curia G, Longo D, Biagini G, Jones RSG, Avoli M. The pilocarpine model of temporal lobe epilepsy. Journal of Neuroscience Methods. 2008. https://doi.org/10.1016/j.jneumeth.2008.04.019 PMID: 18550176

56. Williams PA, White AM, Clark S, Ferraro DJ, Swiercz W, Staley KJ, et al. Development of Spontaneous Recurrent Seizures after Kainate-Induced Status Epilepticus. J Neurosci. 2009 Feb 18; 29(7):2103–12. https://doi.org/10.1523/JNEUROSCI.0980-08.2009 PMID: 19228963

57. Van Nieuwenhuyse B, Raedt R, Sprengers M, Dauwe I, Gadeyne S, Carrette E, et al. The systemic kainic acid rat model of temporal lobe epilepsy: Long-term EEG monitoring. Brain Res. 2015; 1627:1–11. https://doi.org/10.1016/j.brainres.2015.08.016 PMID: 26381287

58. Clifford DB, Olney JW, Maniotis A, Collins RC, Zorumski CF. The functional anatomy and pathology of lithium-pilocarpine and high-dose pilocarpine seizures. Neuroscience. 1987; 23(3):953–68. https://doi.org/10.1016/0306-4522(87)90171-0 PMID: 3437996

59. Viviani B, Bartesaghi S, Gardoni F, Vezzani A, Behrens MM, Bartfai T, et al. Interleukin-1β enhances NMDA receptor-mediated intracellular calcium increase through activation of the Src family of kinases. J Neurosci. 2003 Sep 24; 23(25):8692–700.

4. Danksagung

Mein aufrichtiger Dank geht an Frau Dr. Julika Pitsch, Prof. Dr. Albert Becker und alle Kollegen meiner Arbeitsgruppe, insbesondere Pia Trebing, Phillip Müller und Dr. Silvia Cases Cunillera, für ihre wertvolle Unterstützung während meiner Doktorarbeit.